Brain gyrification in wild and domestic canids: Has domestication changed the gyrification index in domestic dogs?

Jagmeet S. Grewal[1], Tyler Gloe[1], Joseph Hegedus[1], Kathleen Bitterman[1], Brendon Billings[2], Samson Chengetanai[2], Sarah Bentil[3], Victoria X. Wang[4], Johnny C. Ng[4], Cheuk Y. Tang[4], Simon Geletta[5], Bridget Wicinski[6], Mads Bertelson[7], Benjamin C. Tendler[8], Rogier Mars[8,9], Geoffrey K. Aguirre[10], Clare Rusbridge[11,12], Patrick R. Hof[6,13], Chet C. Sherwood[14], Paul R. Manger[2], and Muhammad A. Spocter[1, 2, 15*]

[1] Department of Anatomy, Des Moines University, Des Moines, IA 50312
[2] School of Anatomical Sciences, Faculty of Health Sciences, University of the Witwatersrand, Johannesburg, Republic of South Africa
[3]Department of Mechanical Engineering, Iowa State University, Ames, IA 50011
[4]Departments of Radiology and Psychiatry,and BioMedical and Engineering Imaging Institute, Icahn School of Medicine at Mount Sinai, New York
[5]Department of Public Health, Des Moines University, Des Moines, IA 50312
[6]Nash Family Department of Neuroscience and Friedman Brain Institute, Icahn School of Medicine at Mount Sinai, New York, NY 10029
[7]Center for Zoo and Wild Animal Health, Copenhagen Zoo, Fredericksberg, Denmark.
[8]Wellcome Centre for Intergrative Neuroimaging, FMRIB, Nuffield Department of Clinical Neurosciences, University of Oxford, Oxford, UK
[9]Donders Institute for Brain, Cognition and Behavior, Radboud University Nijmegen, Nijmegen, The Netherlands
[10]Department of Neurology, Perelman School of Medicine, University of Pennsylvania Philadelphia, PA 19104
[11]Fitzpatrick Referrals Orthopedics and Neurology, Fitzpatrick Referrals Ltd, United Kingdom
[12]School of Veterinary Medicine, University of Surrey, Guildford, Surrey, United Kingdom
[13]New York Consortium in Evolutionary Primatology, New York, NY 10124
[14]Department of Anthropology and Center for the Advanced Study of Human Paleobiology, The George Washington University, Washington, DC 20052
[15] College of Veterinary Medicine, Department of Biomedical Sciences, Iowa State University, Ames, IA 50011

Grant sponsor: This work was supported by funding from the Iowa STEM BEST (M.A.S.), the South African National Research Foundation (PRM) and the Carnegie-Wits Alumni Diaspora Program through the Carnegie Corporation of New York (M.A.S. and P.R.M.). The work of R.B.M. is supported by the Biotechnology and Biological Sciences Research Council (BBSRC) UK [BB/N019814/1]. The work of G.K.A. is supported by the Hope for Vision Foundation, Pennsylvania Lion's Foundation. BCT is supported by the Wellcome Trust (202788/Z/16/Z). The Wellcome Centre for Integrative Neuroimaging is supported by core funding from the Wellcome Trust (203139/Z/16/Z).

The Wellcome Centre for Integrative Neuroimaging is supported by core funding from the Wellcome Trust [203139/Z/16/Z].

***Correspondence to:** Muhammad A. Spocter, Ph.D. Department of Anatomy, Des Moines University, 3200 Grand Avenue, Des Moines, IA 50312. Phone: (515) 271-1577, E-mail: Muhammad.spocter@dmu.edu

Number of pages: 43 Figures: 7, Tables: 4.

Associate Editor: Kathleen Rockland

Acknowledgments: We are grateful for MR scan data obtained upon request from Dr. Geoffrey Aguire (Datta et al 2012). We are also grateful for our community partnership with the Des Moines School District (Central Campus) which has helped to foster interest in STEM fields through supporting high school student involvement in our research. We would like to thank Tran Truong and Sandy Le who helped with image capture and interobserver validation.

Data Availability Statement: All quantitative data have been included in the manuscript and imaging data can be provided upon request.

Conflict of Interest: The authors declare no conflicts of interest.

Role of Authors: Study concept and design: MAS, CCS, PRM. Collection of and qualitative analysis of data: JSG, TG, JH, BB, SC, SB, JN, VW, BW, MB, BCT, RM, GKA, CR, PRH, CCS, PRM, MAS. Statistical analysis and interpretation: MAS, SG, CCS, PRM. Procurement, preparation, and fixation of tissue: KB, SC, SB, JN, VW, BW, MB, BCT, RM, GKA, CR, PRH, CCS, PRM, MAS. Obtained funding: MAS, PRM, BCT, RM,

GKA. Drafting of the manuscript: MAS, PRM, CCS, PRH, CR, CYT, BCT, RM. Photomicrography and preparation of figures/tables: JSG, PRM, MAS. Critical revision of the manuscript for important intellectual content: MAS, PRM, CCS, PRH, CR. Study supervision: MAS.

Abstract

Over the last 15 years, research on canid cognition has revealed that domestic dogs possess a surprising array of complex socio-cognitive skills pointing to the possibility that the domestication process might have uniquely altered their brains; however, we know very little about how evolutionary processes (natural or artificial) might have modified underlying neural structure to support species-specific behaviors. Evaluating the degree of cortical folding (i.e., gyrification) within canids may prove useful, as this parameter is linked to functional variation of the cerebral cortex. Using quantitative magnetic resonance imaging to investigate the impact of domestication on the canine cortical surface, we compared the gyrification index (GI) in 19 carnivore species, including six wild canid and 13 domestic dog individuals. We also explored correlations between global and local GI with brain mass, cortical thickness, white and grey matter volume and surface area. Our results indicated that GI values for domestic dogs are largely consistent with what would be expected for a canid of their given brain mass, although more variable than that observed in wild canids. We also found that GI in canids is positively correlated with cortical surface area, cortical thickness and total cortical grey matter volumes. While we found no evidence of global differences in GI between domestic and wild canids, certain regional differences in gyrification were observed.

Key words: canids; domestication; scaling; gyrification; dogs, white matter; evolution, grey matter, RRID:SCR-005988; RRID:SCR-007354.

1. INTRODUCTION

A recent resurgence of interest in the behavior of domestic dogs (Hare et al., 1998; Hare & Tomasello, 2005; McKinley & Sambrook, 2000; Miklosi et al., 1998; Brauer et al., 2006; Anderson et al 1995; Itakura et al., 1998; Hare et al., 2002; Miklosi et al., 2003; Agnetta et al., 2000) has led some to argue that the process of domestication may have uniquely shaped the structure and function of the brain (Hare et al., 1998; Hecht et al., 2019). In this regard, comparative neuroanatomical studies provide an important context for evaluating changes in the neural substrates of canid behavior. Of the limited comparative data available to address this question, some of the earliest studies have indicated that dogs possess a diminished overall brain size and increased variability in brain size relative to their wolf ancestors (Rohrs & Ebinger, 1978; Schleifenbaum, 1973), a pattern consistent with that observed for other domesticated species (Kruska, 1975; Kruska & Schott, 1977; Leybold, 2000; Schuchaer, 1963; Kruska, 1970; 1972; 1973; Kruska & Stephan, 1973; Schleifenbaum, 1973; Kruska, 1980: Ebinger, 1974: Plogman & Kruska, 1990). Although limited in scope, recent allometric analyses have suggested that domestic dogs (i.e., golden retriever) might possess a larger number of cortical neurons when compared to other larger-brained carnivores (Jardim-Messeder et al., 2017). Spocter et al. (2018) recently reported increased variability in canine corpus callosum morphology and demonstrated that amidst the general pattern of conservation in corpus callosum proportions among the canids, there still remained evidence of breed-specific patterning in dogs, likely influenced by artificial selection. More recently, Hecht et al. (2019)

provided additional evidence for the influence of artificial selection on canine brains through observations of breed-specific specializations in brain networks. Using structural MR imaging the authors showed that the anatomy of these brain networks in domestic dogs, correlates with behavioral specializations such as guarding, companionship and scent hunting and that this neuroanatomical variation likely resulted from selective breeding (Hecht et al. 2019).

Collectively these studies highlight the need for additional comparisons of brain morphology across the Canidae to help identify the potential impact of domestication within this group. One measure that might prove informative in the context of canid domestication is the degree of cortical folding (i.e., gyrification). The gyrification index (GI) is a measure of the total cortical surface area relative to the covex smooth hull that defines the outer boundaries of the cerebreum. Across mammalian species, GI is positively correlated with brain size, with larger brained species tending to have more folded cortices (e.g., Manger et al., 2012; Pillay & Manger, 2007). In humans, gyrification differences have been directly linked to cognition, including correlations between frontal gyrification and executive control tasks (Gautam et al. 2015; Gregory et al. 2016; Luders et al. 2008) as well as correlations with altered connectivity in various disoders such as autism spectrum disorder (Shaer et al. 2013) and schizophrenia (Matsuda & Ohi, 2018). Given observations of differences in cognition within the canidae (reviewed in Bensky, Gosling, & Sinn, 2013; Lea & Osthaus, 2018), cerebral folding differences also likely reflect cortical function within this group. This point is perhaps best exemplified by the impairment in cortical function and aberreant behavior observed in domestic dogs with abnormal gyrification as is seen with polymicrogyria in standard poodles (Jurney et al. 2009).

Dogs, however, like all domestic varieties, have undergone a rapid reduction in brain size, by about 30%, since their divergence from wolf-like ancestors, suggesting that GI values should have decreased in parallel with brain size. To date, however, no study has explicitly compared scaling relationships of GI in wild and domestic canid species to evaluate if domestication resulted in any concomitant restructuring of cortical folding patterns. Thus, the present study is aimed at examining the scaling of the GI relative to brain size in carnivores, focusing on wild and domestic canids.

2. MATERIALS AND METHODS

2.1. Specimens

This dataset consists of 80 subjects, representing 42 eutherian mammalian species (of which there are 19 carnivores, including six wild canid species and onne domestic canid varietyie). Of the six wild canid species included in this study, five of the specimens were raised in captivity, while the red fox was wild caught with tissue donated to M.A.S by a local taxidermist. Data were derived from two major sources: 1) primary data obtained through magnetic resonance imaging (MRI) of whole brain scans; and 2) published data of mammalian GI collated from the literature. A complete species list and relevant sources used in this study is included in Table 1. Below we provide an overview of the image acquisition process.

Table 1: Species list, associated brain mass data, global gyrification index (GI), and sources included in the current study. 1 = current study, 2 = Manger et al., 2012, 3 = Pillay & Manger, 2007; 4 = Wosinki et al., 1996; 5 = Zilles et al., 1989.

Order	Species	Common name/Specimen Number	Brain mass (g)	GI	Source
Carnivora	*Mustela erminea*	Ermine	4.0	1.33	2
Carnivora	*Musteal putorius*	European polecat	8.3	1.36	2
Carnivora	*Neovison vison*	American mink	8.5	1.46	2
Carnivora	*Cynictis penicillata*	Meerkat	14.5	1.35	3

Carnivora	*Bassariscus astutus*	Ringtail	20.7	1.46	2
Carnivora	*Galictis vittata*	Greater grisson	24.3	1.59	2
Carnivora	*Felis catus*	Domestic cat	36.9	1.5	3
Carnivora	*Nasua narica*	White nosed coati	37.0	1.62	2
Carnivora	*Ailurus fulgens*	Lesser panda	41.7	1.51	2
Carnivora	*Crocuta crocuta*	Hyena	162.5	1.74	3
Carnivora	*Pathera leo*	African lion	258.0	1.85	3
Carnivora	*Ursus maritimus*	Polar bear	458.6	2.04	3
Carnivora	*Vulpes vulpes*	Red fox	44.0	1.66	2
Carnivora	*Panthera tigris*	Siberian tiger/ PT1	233.6	1.91	1
Carnivora	*Panthera tigris*	Bengal Tiger/ PT2	187.3	1.91	1
Carnivora	*Felis catus*	Domestic cat/ FC1	31.0	1.71	1
Carnivora	*Lycaon pictus*	African wild dog/LP1	125.8	1.74	1
Carnivora	*Lycaon pictus*	African wild dog/LP2	99.7	1.88	1
Carnivora	*Vulpes zerda*	Fennec fox/ VZ1	16.7	1.28	1
Carnivora	*Vulpes vulpes*	Red fox/ VV1	44.8	1.50	1
Carnivora	*Chrysocyon brachyurus*	Maned wolf/ CB1	83.6	1.80	1
Carnivora	*Chrysocyon brachyurus*	Maned wolf/ CB2	92.0	1.82	1
Carnivora	*Canis lupus lupus*	European wolf/ CL1	145.5	2.10	1
Carnivora	*Canis lupus lupus*	European wolf / CL2	133.5	1.77	1
Carnivora	*Canis latrans*	Coyote/ CL1	73.3	1.70	1
Carnivora	*Canis lupus familiaris*	Beagle / CF1	60.9	1.87	1
Carnivora	*Canis lupus familiaris*	Beagle/ CF2	70.9	1.76	1
Carnivora	*Canis lupus familiaris*	Mix Hound /CF3	69.3	2.10	1
Carnivora	*Canis lupus familiaris*	Mix hound/ CF4	59.7	1.85	1
Carnivora	*Canis lupus familiaris*	Cavalier King Charles/ CF5	73.7	1.75	1
Carnivora	*Canis lupus familiaris*	Cavalier King Charles/ CF6	71.6	1.77	1
Carnivora	*Canis lupus familiaris*	Mix hound/ CF7	66.9	1.74	1
Carnivora	*Canis lupus familiaris*	Mix hound/CF8	70.6	1.91	1
Carnivora	*Canis lupus familiaris*	Mix hound/ /CF9	55.9	1.89	1
Carnivora	*Canis lupus familiaris*	Mix hound/CF10	90.6	1.81	1
Carnivora	*Canis lupus familiaris*	Mix hound/CF11	79.8	2.36	1
Carnivora	*Canis lupus familiaris*	Mix hound/CF12	77.9	1.65	1
Carnivora	*Canis lupus familiaris*	Mix hound/CF13	71.5	1.94	1
Carnivora	*Canis lupus familiaris*	Dachsund	47.4	1.61	4
Carnivora	*Canis lupus familiaris*	Dachsund	59.7	1.55	4
Carnivora	*Canis lupus familiaris*	Dachsund	61	1.65	4
Carnivora	*Canis lupus familiaris*	Pekin	47.8	1.66	4
Carnivora	*Canis lupus familiaris*	German Sheep-dog	85.7	1.73	4

Carnivora	*Canis lupus familiaris*	German Sheep-dog	95.5	1.66	4
Carnivora	*Canis lupus familiaris*	German Sheep-dog	90.1	1.68	4
Carnivora	*Canis lupus familiaris*	Dobermann	109	1.67	4
Carnivora	*Canis lupus familiaris*	Fox terrier	68.1	1.63	4
Carnivora	*Canis lupus familiaris*	Mix	55	1.62	4
Carnivora	*Canis lupus familiaris*	Mix	61.2	1.6	4
Carnivora	*Canis lupus familiaris*	Mix	59.3	1.59	4
Carnivora	*Canis lupus familiaris*	Vizsla /Hungarian pointer	112.2	1.83	4
Carnivora	*Canis lupus familiaris*	Spitz	85.8	1.62	4
Carnivora	*Canis lupus familiaris*	Terrier	90.1	1.77	4
Carnivora	*Canis lupus familiaris*	Terrier	99.2	1.69	4
Carnivora	*Canis lupus familiaris*	Terrier	75.3	1.63	4
Carnivora	*Canis lupus familiaris*	Poodle	66.8	1.58	4
Carnivora	*Canis lupus familiaris*	Beagle	70.2	1.58	4
Carnivora	*Canis lupus familiaris*	Pinscher	56.2	1.54	4
Primates	*Nycticebus coucang*	Slow loris	13.35	1.31	5
Primates	*Aotus trivirgatus*	Owl monkey	18	1.26	5
Primates	*Eulemur mongoz*	Mongoose lemur	21.8	1.33	5
Primates	*Saimiri sciureus*	Squirrel monkey	22.68	1.56	5
Primates	*Macaca mulatta*	Rhesus monkey	90	1.75	5
Primates	*Mandrillus sphinx*	Mandrill	155.9	2.18	5
Primates	*Pan troglodytes*	Chimpanzee	405.5	2.3	5
Primates	*Homo sapiens*	Human	1400	2.99	5
Artiodactyla	*Sus scrofa domesticus*	Domestic pig	95.3	2.16	5
Artiodactyla	*Odocoileus virginianus*	White-tailed deer	160	2.27	5
Artiodactyla	*Lama glama domesticus*	Llama	200.3	2.7	5
Artiodactyla	*Bos taurus indicus*	Zebu	474	2.53	5
Artiodactyla	*Equus burchellii*	Zebra	520.5	2.94	5
Rodentia	*Mus musculus*	Mouse	0.65	1.03	5
Rodentia	*Mesocricetus auratus*	Hamster	0.9	1.01	5
Rodentia	*Rattus norvegicus*	Rat	2.48	1.02	5
Rodentia	*Dasyprocta leporina*	Agouti	17.2	1.23	5
Rodentia	*Hydrochaeris hydrochaeris*	Capybara	51	1.3	5
Rodentia	*Castor canadensis*	North American beaver	38.5	1.02	5
Afrotheria	*Loxodonta africana*	African elephant	5076.7	3.89	2
Afrotheria	*Procavia capensis*	rock hyrax	16	1.38	2
Afrotheria	*Trichechus manatus*	West Indian manatee	350	1.07	2

160

161

162 **2.2. MRI acquisition**

163 Magnetic resonance imaging was performed on the whole brains of 19 carnivore species
164 and resulting GI data was combined with that collated from the literature (see Table 1). All
165 scanning was carried out in strict accordance with the recommendations in the Guide for the
166 Care and Use of Laboratory Animals of the National Institutes of Health and approved by the
167 Institutional Animal Care and Use Committees of the University of Pennsylvania (IACUC
168 Protocol #s 803269 and 801870) and Des Moines University, as well as the Animal Ethics and
169 Screening Committee (AESC) of the University of the Witwatersrand (AESC No. 2012/53/01).
170 MR images were obtained through ongoing collaborations with four imaging sources: 1) the
171 Department of Radiology, Icahn School of Medicine at Mount Sinai; 2) the University of Surrey
172 and Fitzpatrick Referrals Ltd Image database; 3) the MRI image data repository of Dr. Geoffrey
173 Aguire at University of Pennsylvannia; and 4) the Department of Radiology at Oxford
174 University. Representative images from each of these imaging sources is shown in Figure 1.
175 Scanning undertaken at the Icahn School of Medicine was performed using a 7 T Bruker
176 Biospec MR System. The brains of specimens LP1 -LP3, CF1-CF4, CB1, CB2, CL1, VV1,
177 VZ1, PT1, PU1 were removed within 14 hours of death and immersion fixed in 10% formalin at
178 necropsy before being transferred to a solution of 0.1 M phosphate buffered saline (PBS) with
179 0.1% sodium azide solution and stored at 4°C prior to scanning. A 3D FLASH (fast low angle
180 shot) sequence was used with parameter settings of: TR (time to repetition) = 36 ms, TE (time
181 to echo) = 23 ms, flip angle = 15°, FOV (field of view) = 128×128×175, matrix size =
182 384×384×384 mm in each slab, 20 averages, slice thickness = 0.5mm, scan resolution was 0.30
183 mm isotropic. The scanning at Fitzpatrick Referrals Ltd was performed using a 1.5 T Siemens

machine (Symphony, Erlangen, Germany), T2 weighted were obtained from specimens CF4 and CF5 with parameter settings of: TR = 3450 ms, TE = 95 ms, flip angle=150°, FOV = 384× 384×15 mm in each slab, matrix size = 320x323, slice thickness = 1.5 mm, scan resolution was 0.43 mm isotropic.

Scan data obtained from Dr. Geoffrey Aguire formed part of a prior study on the canine brain. Scanning was performed on a 7~~3~~ T Siemens Trio machine (Erlangen, Germany) and T1-weighted images were obtained from seven anesthetized canids (CF6 -CF13). T1 weighted MPRAGE image sequences were acquired with parameter settings of: TR = 3 s, TE = 3.4 ms, flip angle = 12°, FOV = 84×84×34.3 mm in each slab, matrix size = 256×256×104, scan resolution was 0.33 mm isotropic. A detailed outline of this scanning protocol ~~was~~ was previously published (Datta et al 2012). Scanning undertaken at Oxford University was performed using a 7 T Bruker Biospec MR System. Following overdose with sodium pentobarbital (200 mg/kg, i.v., the head of animal CL1 (European wolf) was perfusion fixed in 2 l of 4% paraformaldehyde in 0.1M phosphate buffer (PB). The brains were then postfixed in 4% paraformaldehyde in 0.1M PB for 48 h before storage in freezer storage solution. Scanning was performed at the Wellcome Centre for Integrative Neuroimaging, Nuffield Department of Clinical Neurosciences, University of Oxford. The specimen was scanned on a Siemens 7T whole body scanner (28ch-recieve/1ch-transmitl knee coil - QED). A high resolution structural scan was acquired using a true fast imaging with steady-state free-precession (TRUFI) sequence ~~(resolution = 0.22 x 0.22 x 0.22 mm^3, flip angle = 30 degrees, TE = 7.33 ms,~~ TR = 14.65 ms, TE = 7.33 ms, ~~bandwidth = 100 Hz/pixel,~~ flip angle = 30°, ~~matrix size = 542 x 736 x448,~~ FOV = 118 x 160 x 99 mm in each slab^~~3~~, matrix size = 542 x 736 x448, scan resolution was 0.22 mm isotropic. ~~, 1 average, phase increment = 90 degrees).~~

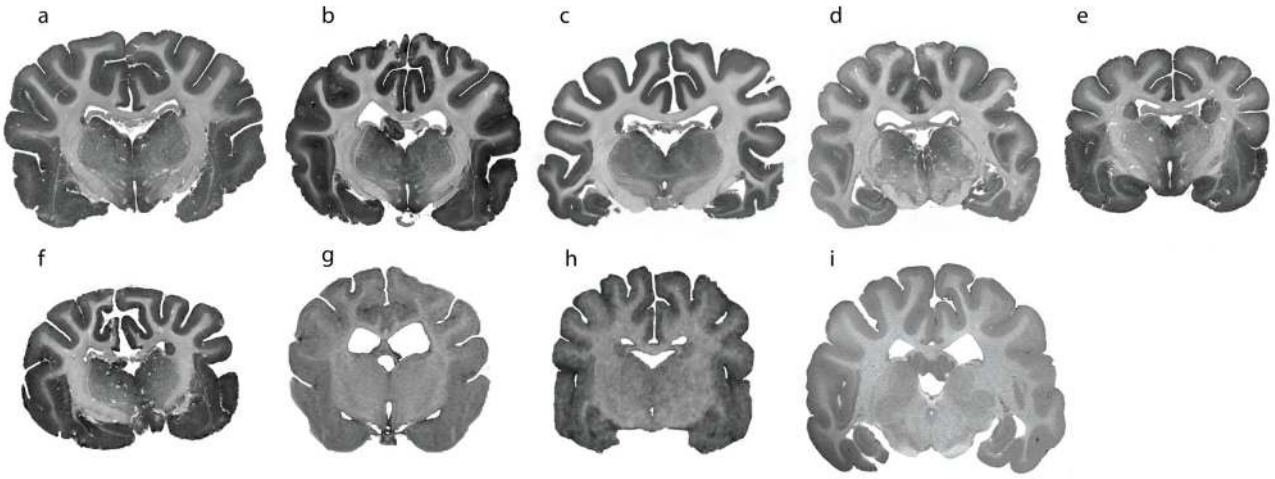

Figure ~~1~~1: Representative coronal images through the diecephalon of select canid species used in the current study. **a** = African wild dog; **b** = Domes~~te~~tic dog; **c** = Maned wolf; **d** = coyote; **e** = red fox~~*Vv*~~; **f** = fennec fox~~*V*~~; **g** = domestic dog; **h** = domestic dog; **i** = European wolf. Scan **a- f** were obtained through scanning at the Department of Radiology, Icahn School of Medicine at Mount Sinai. Scan **g** is that of a domestic dog (Cavalier King Charles spaniel) scanned through collaboration with the University of Surrey and Fitzpatrick Referrals Ltd. Scan **h** is that of a domestic dog acquired through the MRI image data repository of Dr. Geoffrey Aguire at University of Pennsylvannia. Scan **i** was acquired through collaboration with the Department of Radiology at Oxford University.

224

225 **2.3. MR Image preprocessing and segmentation pipeline**

226 Following MR image aqusition, the resulting DICOMS were loaded into Analyze
227 Version 10.0 (www.analyzedirect.com, RRID:SCR-005988) for postprocessing. The
228 postprocessing step involved ~~standardizing MR image resolution (to minimize methodological~~
229 ~~differences and ensure allometrically similar spatial resolutions between species) followed by~~
230 resectioning the image sequences along the A-P plane to facilitate import into BrainVisa
231 (http://brainvisa.info/web/index.html, RRID:SCR-007354). Preprocessed MR images were
232 loaded into BrainVisa for subsequent grey and white matter segmentation and surface
233 reconstruction. The processing steps performed in BrainVisa are summarized in Figure ~~1~~ 2 and
234 are derived from a similar pipeline created for the human brain and freely distributed as a
235 BrainVisa toolbox (http://brainvisa.info; Mangin et al., 2004).

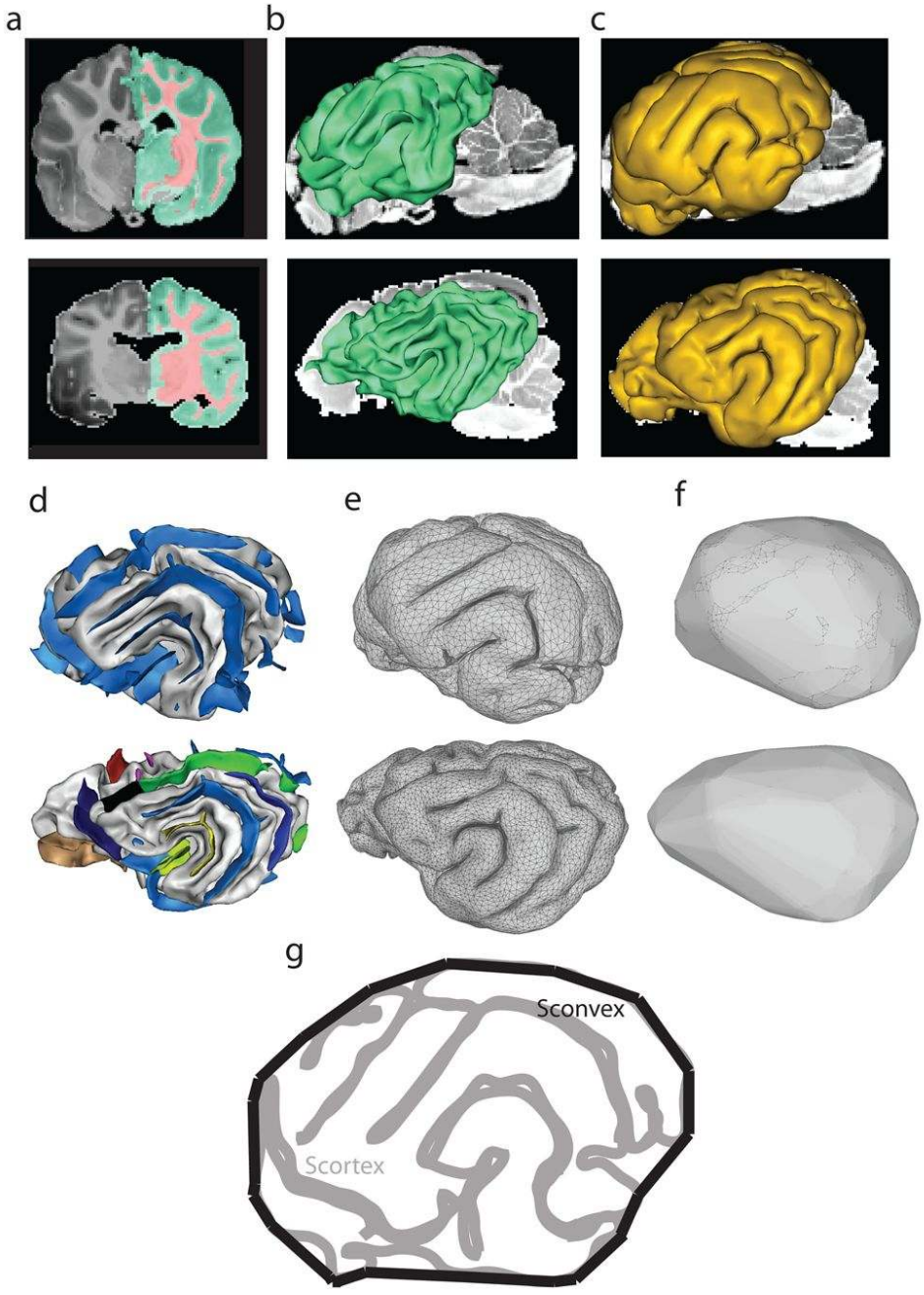

Figure ~~1~~2: Representative images showing 3D data from the domestic dog (first row) and European wolf (second row). The series of images outlines the image segmentation pipeline used in calculating the gyrification index in both species. In Step 1 of processing, the MR images are imported into BrainVisa where the Morphologist tool is used to delineate the grey and white matter subcomponents, followed by pial and white matter reconstruction and sulcal extraction (**a-d**). In Step 2, the pial and white matter mesh data is imported into MeshLab (**e-f**),

where the GI is calculated as the ratio of the the surface area of the outer cerebral cortex (Scortex) divided by the surface area of the convex hull of the cerebral cortex(Sconvex) (**g**).

After an initial pilot study, tuning of the pipeline was undertaken to account for differences in carnivore anatomy as well as heterogeneity of the acquired *in vivo* and postmortem scan protocols. For the post mortem scans, intensities were inverted to correspond to white and grey matter before running the data through the Morphologist pipeline of BrainVisa. For the *in vivo* scan data, skull stripping was performed on each MRI volume using the deformable suface based algorithm as implemented by the Brain Extraction Tool (BET) included with the MRIcro software (https://people.cas.sc.edu/rorden/mricro/mricro.html, RRID:SCR-008264). In brief, the segmentation processing steps as implemented in BrainVisa included correction of spatial inhomogeneities, global spatial normalization (Mangin 2000), automatic analysis of the signal histogram and creation of a binary brain mask, splitting of the brain mask into corresponding hemispheres and cerebellum (Mangin et al., 1996), and the extraction of the gray/white interfaces (see Fig.~~1a~~2a) (Mangin et al., 1995; Mangin et al., 2004) from the tissue segmented images to create 3D white matter and pial surface reconstructions (see Fig. ~~1b~~2b-f). The resultant 3D reconstructions were then saved as stereolithographic files before being imported into the open source mesh editing software Meshlab (http://www.meshlab.net/, RRID:SCR-003430).

2.4. Computing the gyrification index from 3D mesh data

2.4.1 The global gyrification index

Stereolithographic mesh files were opened in Meshlab and the surface area and volume for each mesh was computed (T.G) using the built~~d~~-in Quality Measures and Computations

Filter. To calculate the GI, we used a surface based approach similar to that applied in previous studies of the non-human primate brain (e.g., Rogers et al., 2010). This approach adapts the ~~classical~~ 2D histological method of Zilles et al. (Zilles et al., 1989; Zilles et al., 1988) to a 3D framework. In accordance with this approach, GI was calculated as the ratio of the surface area of the pial surface (i.e., outer gyrated surface, Scortex) and the area of its convex hull (i.e., Sconvex; see Fig. ~~1g~~2g-i). The convex hull for each pial surface was constructed in Meshlab by applying the Remeshing, Simplification and Reconstruction Filter. The global GI was calculated by computing the GI for each hemisphere and then averaging this to obtain a single value for a given subject. In addition to the computation of global GI from 3D mesh data, we also combined data from published reports (Manger et al., 2012; Zilles et al., 1988; Wosinki et al., 1996) to establish a comprehensive overview of GI scaling in carnivores. Caution was taken to ensure that all reported species values were internally consistent between sources. Recent studies in mammals have helped validate the use of both 2D and 3D data with broad alignment demonstrated between histological and MRI imaging data (e.g., Leergaard et al., 2010; Seehaus et al., 2015) and particular congruency in GI measures obtained from 2D and 3D approaches (e.g., Rogers et al., 2010). A complete table of the global GIs for all the specimens, is shown in Table 1. Global GIs and associated cortical thickness and grey matter surface area calculated at a hemispheric level, is shown in Table 2 for the canid subset.

Table 2: Global gyrification index (GI), Total cortical grey matter surface area (mm^2), Total cortical grey matter volume (mm^3) and cortical grey matter mass (g) and cortical thickness (mm) for seven canid species.

Species	Brain mass (g)	Total Cortical Grey Surface area (mm^2)	Total Cortical Grey Volume (mm^3)	Total Cortical Grey mass (g)	Global GI	Cortical Thickness (mm)
Maned wolf	87.8	18079.27	67441.94	67.44	1.81	2.10
Red fox	44.8	12729.45	33565.77	33.57	1.50	1.86

Fennec fox	16.7	5478.44	12017.13	12.02	1.28	1.76
African wild dog	112.8	29921.41	90737.56	90.74	1.83	2.40
Coyote	73.3	20261.88	56014.72	56.01	1.70	1.94
European wolf	133.5	33233.37	96746.93	96.75	1.77	2.15
Domestic dog	70.9	10311.82	55575.65	55.58	1.73	2.01

2.4.2 The local gyrification index, white and gray matter volumes, surface area and cortical thickness

To evaluate the existence of potential regional differences in GI and correlated changes in white and gray matter, we computed the local GI in a subset of our original sample (see Table 3).

Table 3: Local gyrification index (lGI), grey and white matter cortical surface area (mm^2), grey and white matter cortical volume (mm^3) and local cortical thickness (mm) for select canid species. All measurements were completed in one hemisphere (left), unless otherwise indicated.

Species	Region	Grey matter surface area (mm^2)	Grey matter volume (mm^3)	White matter surface area (mm^2)	White matter volume (mm^3)	Local GI	Local cortical thickness (mm)
Domestic dog	Frontal	1708.13	2875.42	612.56	365.71	1.16	1.68
Red fox	Frontal	944.23	1604.17	599.83	324.16	1.01	1.7
European wolf	Frontal	2947.24	5582.99	1118.37	796.2	1.24	1.89
Maned wolf	Frontal	1968.13	3899.32	1968.13	3899.32	1.18	1.98
Coyote	Frontal	1769.61	2990.94	621.55	395.91	1.26	1.69
African wild dog	Frontal	2669.13	5497.72	1128.16	1085.88	1.19	2.06
Domestic dog	PT1	4233.18	9761.23	2138.45	1919.2	1.42	2.31
Red fox	PT1	1638.5	3645.64	1298.82	945.78	1.11	2.22
European wolf	PT1	4937.97	11701.03	2385.13	2548.72	1.36	2.37
Maned wolf	PT1	4475.86	9762.58	2443.2	2827.76	1.46	2.18
Coyote	PT1	5063.42	11633.86	1815.34	1479.76	1.55	2.3
African wild dog	PT1	5988.73	14012.14	3126.55	3841.12	1.47	2.34
Domestic dog	PT2	5206.18	11509.5	4002.14	3162.7	1.55	2.21
Red fox	PT2	3889.48	8312.88	1999.99	1644.41	1.55	2.14

European wolf	PT2	8905.61	19844.18	3786.42	4701.09	1.76	2.23
Maned wolf	PT2	7378.68	16378.42	3893.73	4200.7	1.78	2.22
Coyote	PT2	4612.31	8910.67	3159.61	2921.01	1.57	1.93
African wild dog	PT2	8366.19	22495.15	5890.24	6559.8	1.62	2.69
Domestic dog	Occ	1857.83	3422.35	1366.96	862.91	0.67	1.84
Red fox	Occ	984.37	1350.75	1117.32	730.66	1.09	1.37
European wolf	Occ	4090.3	8776.46	1956.37	1979.72	1.39	2.15
Maned wolf	Occ	2259.2	4489.16	1474.34	1317.01	1.17	1.99
Coyote	Occ	2175.81	4018.12	1512.22	1092.23	1.2	1.85
African wild dog	Occ	3224.79	8084.34	2548.38	2591.46	1.21	2.51

Using the 3D slicing tool Slic3r (https://slic3r.org/, RRID:SCR-002315) we partitioned the pial and white matter mesh of each subject into anatomical subcomponents (see Fig. ~~2~~3) and computed the local GI along with the associated white, gray matter volume and surface area for each subregion.

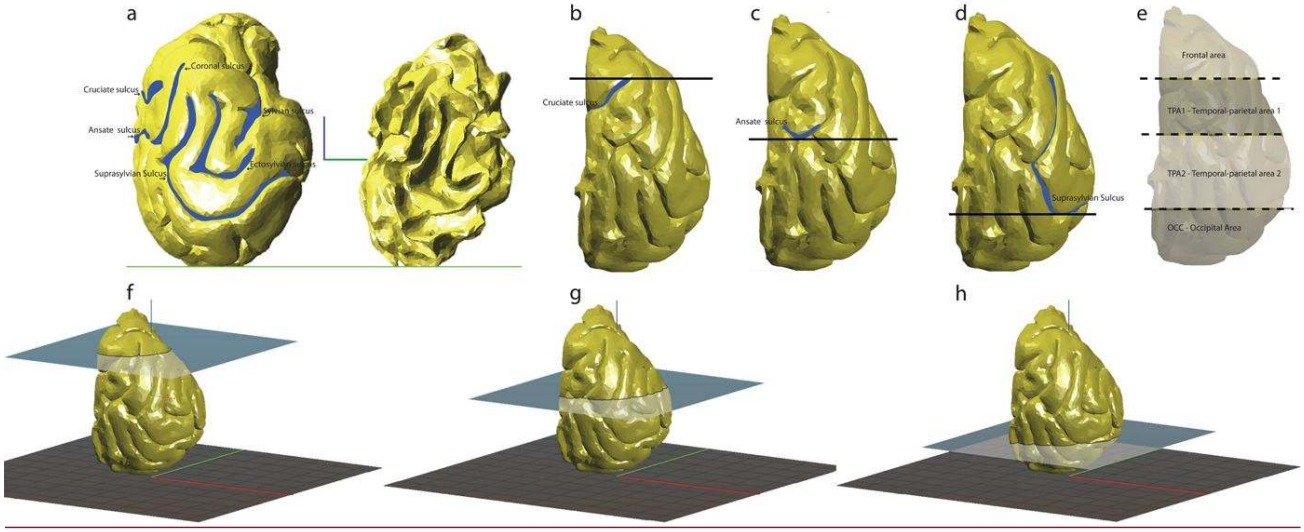

Figure ~~2~~3: Representative lateral and dorsolateral images of the maned wolf brain showing the 3D partitioning approach used for slicing the 3D mesh data (i.e., grey and white matter surfaces) into anatomical subregions (frontal, TPA1, TPA2, OCC). To standardize the processing approach, each subject mesh file was vertically aligned in Slic3r and sectioned using the Cutting Tool. Cutting planes were placed perpendicular to the long axis of the vertically aligned hemisphere and anatomically defined sulcal landmarks were used for partitioning (**a-e**). Dorsal lateral views of the maned wolf brain showing screenshots of the vertical alignment and virtual sectioning/slicing tool of the hemisphere (**f- h**). After reslicing the pial mesh into

subcomponents, the local GI (lGI) was calculated using the ratio of the pial surface area (in the region of interest) and the surface area of the convex hull for the subregion.

We used a pragmatic approach to partition the mesh files using available cortical maps of carnivore brains (Sereno & Allman, 1991; Manger et al., 2008; Kroenke et al., 2014; Chengetenai et al., 2020) and also basing our anatomical landmarks on the consistency with which these areas could be partitioned from the cortical surface across carnivore species. Figures ~~2~~ 3 and ~~3~~ 4 present an overview of our landmark designations and correspondence with the available functional and/or cytoarchitectural maps in the ferret, cat and African wild dog. In the absence of available functional data for all the canids in our sample, this approach provides a reasonable guide to interpret potential regional folding differences. To standardize our processing approach, each subject mesh file was vertically aligned in Slic3r with the occipital lobe resting on the planar X-Y surface and the medial surface projecting vertically upright, perpendicular to the Z- axis (Fig. ~~2a~~ 3a) and sectioned using the Cutting Tool based on the placement of uniform anatomical landmarks. The pial and white matter mesh for each subject was subsequently partitioned into four anatomical subregions: 1) a frontal area (F), defined as all the region rostral to a tangent passing through the most anterior projecting point of the cruciate sulcus (Fig. ~~2b~~3b, e, g); an anterior temporoparietal area (TPA1), defined as the region located between the anterior projecting point of the cruciate sulcus and the most posterior projecting point of the ansate sulcus (Fig. ~~2c~~3c, e); the posterior temporoparietal area (TPA2) defined as the region located between the most posterior projecting point of the ansate sulcus and a tangent drawn through the most posterior projecting point of the suprasylvian sulcus (Fig. ~~2d~~3d, e, h); and an occipital area (OCC) defined as the region caudal to a tangent drawn through the most posterior projecting point of the suprasylvian sulcus (Fig. ~~2d~~3d, e, h). After reslicing

the pial mesh into subcomponents, the local GI was calculated using the ratio of the pial surface area in the region of interest (i.e., F, TPA1, TPA2, OCC) and the surface area of the convex hull for the subregion.

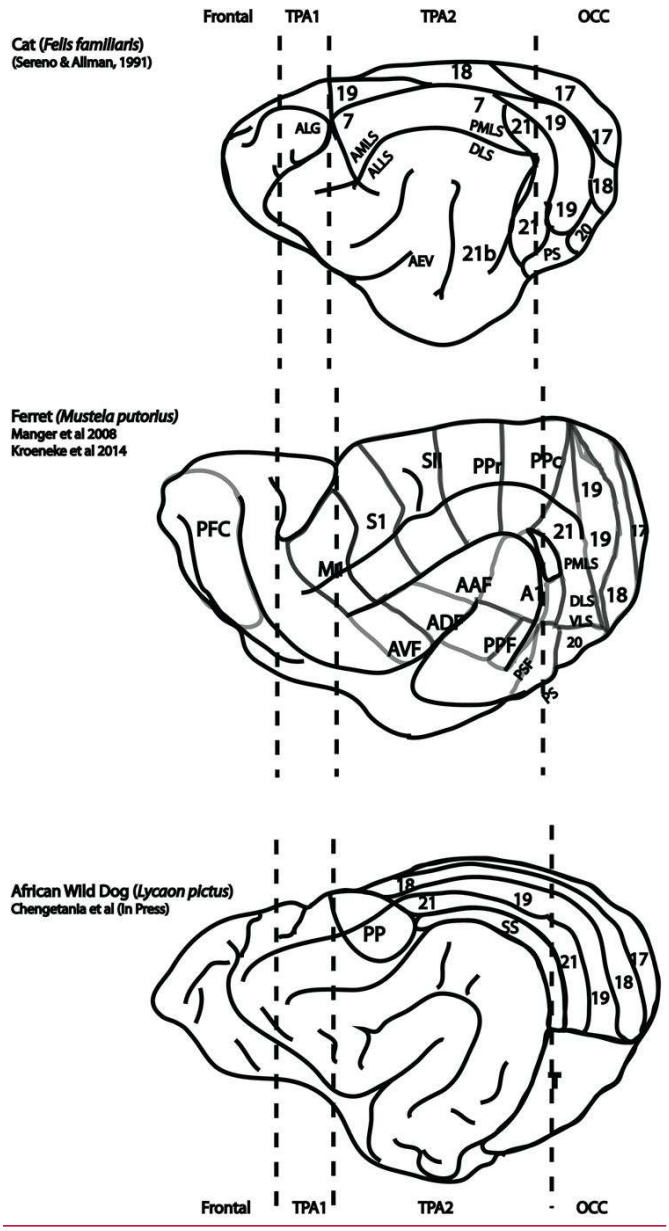

Figure ~~34~~: Comparative cortical maps of three closely related carnivore species, the domestic cat (Sereno & Allman, 1991), ferret (Manger et al 2008; Kroeneke et al., 2014) and African wild dog (Chengetania et al. 2020). The dashed vertical lines indicate the placement of the four

anatomical regions (frontal, TPA1, TPA2, OCC) from which local gyrification indices were sampled in the current study. Note the images are not drawn to scale.

To validate our approach, a pilot study was conducted on three randomly selected hemispheres by two observers (T.G.~~V.K.~~ and M.A.S). Each observer was responsible for independently aligning and orientating the mesh file in Slic3r, followed by placement of the slicing plane and computing the resulting surface area and volume in Meshlab. Interobserver congruency was assessed using the concordance correlation coefficient of reproducibility (Lin, 1989). Results from this pilot study indicated a high congruency in surface area and volume measures obtained by the two observers (i.e., > 90), suggesting that the area definitions were reproducible and covaried in a systematic fashion.

We computed cortical thickness (local and global) for each specimen used in the canid sub-sample. Cortical thickness was measured in accordance with the approach used by Mota & Herculano-Houzel (2015), where cortical thickness is computed as the grey matter mesh volume divided by grey matter mesh surface area.

2.5. Data analysis

The statistical analysis was implemented with four main goals in mind. To evaluate: 1) whether domestic dogs underwent any relative changes in global GI in comparison to other carnivores and canids (i.e., wolves, foxes and coyotes); 2) the nature of intraspecific scaling of global GI within a sample of domestic dogs; 3) the contribution of grey and white matter differences to interspecific variation in local GI; and 4) scaling relationships between local GI and grey matter surface area and cortical thickness. With this in mind, we used a combination of Ordinary Least Squares (OLS) regression analysis and Phylogenetic Generalized Least Squares

369 (PGLS) to evaluate the scaling of GI against brain mass. We applied PGLS and OLS to
370 interspecific comparisons of GI within Mammalia, Carnivora and Canidae, while OLS was used
371 to evaluate intraspecific scaling within the domestic dogs. All statistical analyses were
372 undertaken in R Version 3.4.1 (www.r-project.org/, RRID:SCR-001905) with PGLS being
373 performed using the 'caper' add-on package (Orme et al. 2013). The phylogeny used in the
374 current study is shown in Figure 4-5 as derived from (Bininda-Emonds et al., 2007, 2008;
375 Nyakatura & Bininda -Emonds, 2015).

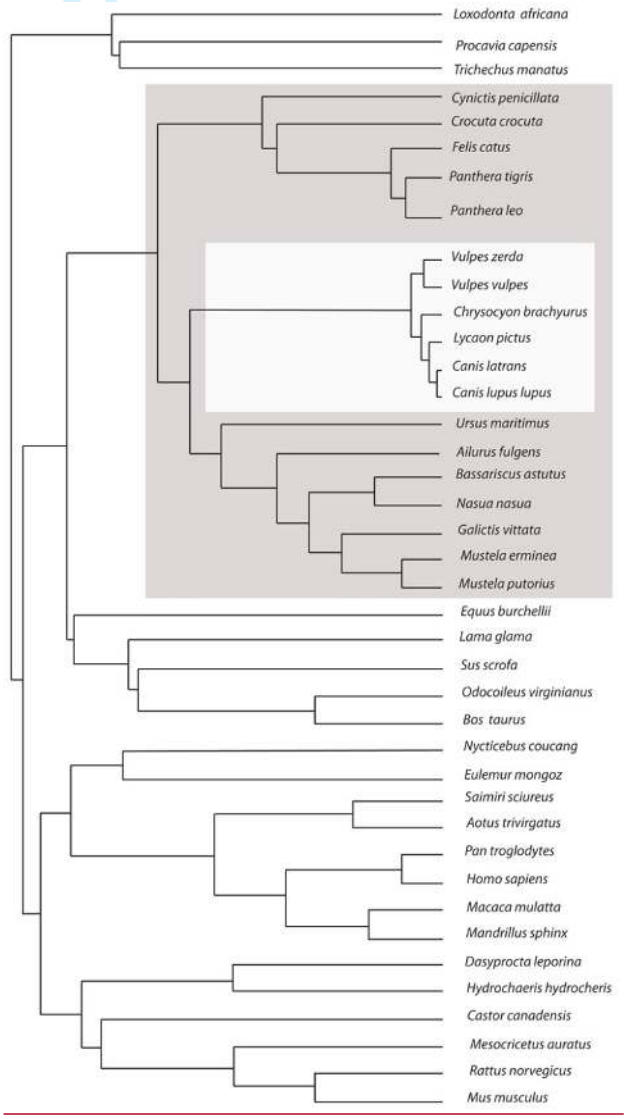

376

Figure 45: Phylogeny used in the implementation of phylogenetic generalized least squares (PGLS). PGLS was performed using the caper package (Orme et al., 2013). The phylogeny was constructed using data based on the mammalian super-tree (Bininda-Edmonds et al., 2007, 2008) and a recent super-tree for the Carnivora (Nyakatura & Bininda-Emonds, 2015).

All confidence and prediction intervals were calculated using OLS regression statistics. Domesticated dogs were excluded from all PGLS regressions but where indicated the canine data points were superimposed on the interspecific regression curves to help visualize the range of canine GI values. The raw data used to derive these relationships are shown in Tables 1-3 and a summary of the regression statistics derived from the analyses is shown in Table 4.

Table 4: Summary of the regression statistics for the gyrification index (Global or local) obtained using phylogenetic generalized least squares regression (PGLS) and ordinary least squares regression (OLS).

Group	Variables (*x*, *y*)	Model	λ	Adjusted R^2	Slope	SE	t-value	Pr(>|t|)	Intercept	SE	t-value	Pr(>|t|)
Mammals	Brain mass, Global GI	OLS		0.687	0.143	0.015	9.424	0.000	-0.029	0.029	-0.999	0.324
Mammals	Brain mass, Global GI	PGLS	0.998	0.676	0.145	0.016	9.078	0.000	-0.046	0.042	-1.108	0.275
Carnivores	Brain mass, Global GI	OLS		0.866	0.102	0.010	10.545	0.000	0.036	0.017	2.102	0.052
Carnivores	Brain mass, Global GI	PGLS	0.00	0.866	0.102	0.010	10.545	0.000	0.036	0.017	2.102	0.052
Canids	Brain mass, Global GI	OLS		0.974	0.194	0.014	13.590	0.000	-0.129	0.026	-4.890	0.008
Canids	Brain mass, Global GI	PGLS	0.00	0.974	0.194	0.014	13.585	0.000	-0.129	0.026	-4.890	0.008
Canines	Brain mass, Global GI	OLS		0.003	0.077	0.074	1.041	0.306	0.095	0.137	0.696	0.492
Canids	Total grey matter surface area, Global GI	OLS		0.842	0.199	0.038	5.261	0.006	-0.629	0.161	-3.920	0.017
Canids	Total grey matter surface	PGLS	0.00	0.842	0.199	0.038	5.261	0.006	-0.629	0.161	-3.921	0.017

	area, Global GI											
Canids	Total grey matter volume, Global GI	OLS		0.942	0.175	0.019	9.083	0.001	-0.605	0.090	-6.697	0.003
Canids	Total grey matter volume, Global GI	PGLS	0.00	0.942	0.175	0.019	9.083	0.001	-0.605	0.090	-6.697	0.003
Canids	Average Cortical thickness, Global GI	OLS		0.676	1.081	0.319	3.382	0.027	-0.117	0.098	-1.185	0.302
Canids	Average Cortical thickness, Global GI	PGLS	0.00	0.676	1.081	0.319	3.382	0.027	-0.117	0.098	-1.185	0.302
Canids	Local grey matter surface area, Local GI	OLS		0.849	0.235	0.023	10.398	0.000	-0.699	0.080	-8.767	0.000
Canids	Local grey matter volume, Local GI	OLS		0.776	0.189	0.023	8.166	0.000	-0.597	0.089	-6.704	0.000
Canids	Local white matter surface area, Local GI	OLS		0.605	0.221	0.040	5.487	0.000	-0.595	0.132	-4.505	0.000
Canids	Local white matter volume, Local GI	OLS		0.500	0.145	0.032	4.475	0.000	-0.343	0.106	-3.244	0.005
Canids	Local cortical thickness, Local GI	OLS		0.272	0.599	0.210	2.848	0.011	-0.062	0.068	-0.908	0.376

3. RESULTS

3.1. Interspecifc scaling of global GI with brain mass across mammals and within the carnivores

Ordinary least squares regression analysis (OLS) and PGLS revealed a strong hypoallometric relationship between brain mass and GI in mammals (OLS slope = 0.14, $p <$ 0.001, R-squared = 0.70; PGLS slope = 0.14, $p < 0.001$, R-squared = 0.68). This pattern of allometry was also observed for interspecific comparisons of GI within the Carnivora (OLS slope = 0.10, $p < 0.001$, R-squared = 0.87; PGLS slope = 0.10, $p < 0.001$, R-squared = 0.87). (Fig. ~~5a~~6a, b). Lambda values for the mammalian regression line indicated the presence of a phylogenetic signal in the data (i.e., $\lambda > 0$), whereas the lambda values for the carnivores and canids indicated a low phylogenetic signal (Table 4).

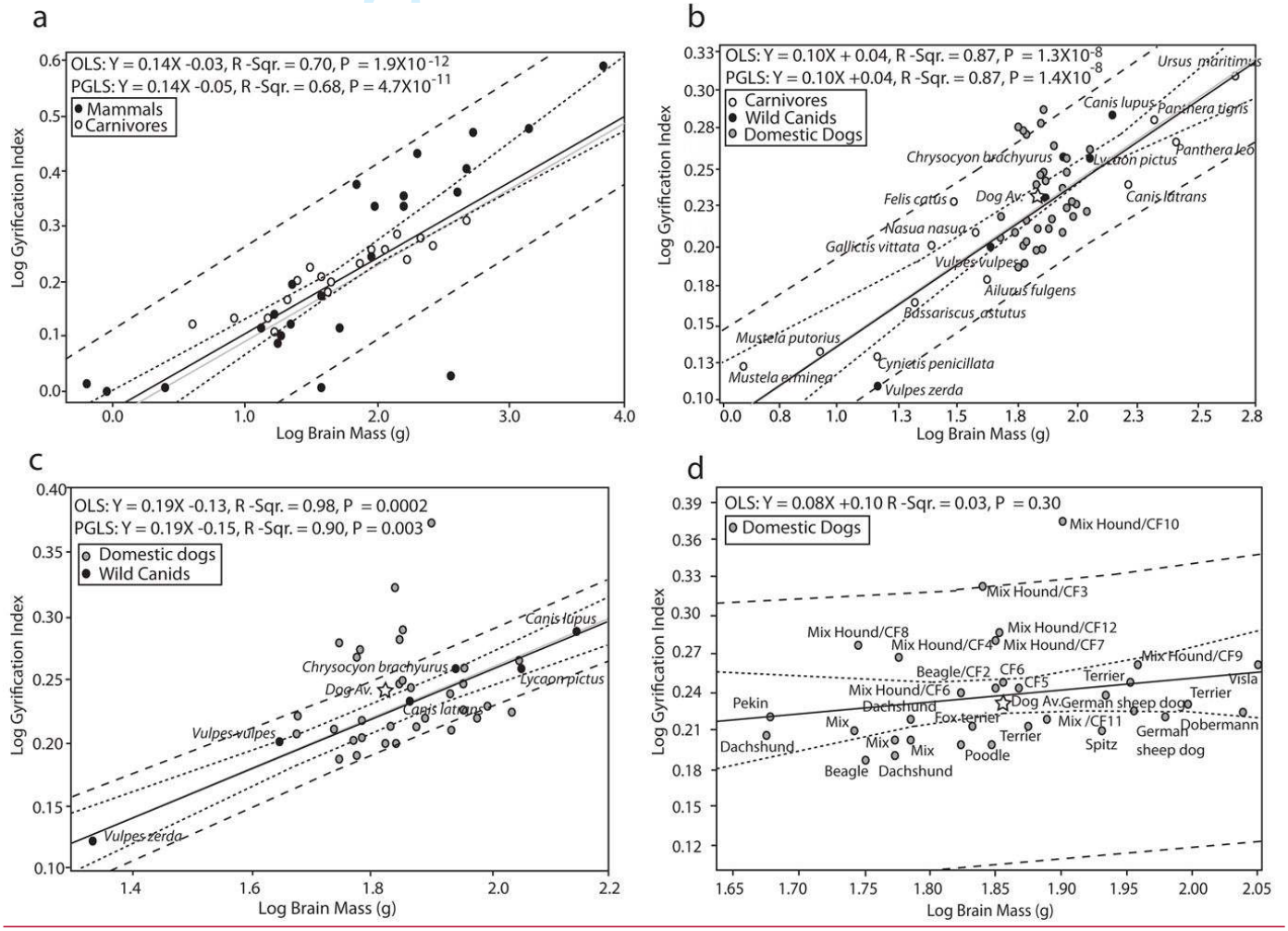

Figure ~~5~~6: Regression analysis of the gyrification index (Global) plotted against brain mass in a range of mammals. All data were logarithmically transformed (base 10) prior to inclusion in the regression analyses. Data used to derive these relationships are shown in Table 1. OLS = ordinary least squares regression; PGLS = phylogenetic generalized least squares. OLS lines are plotted in black, PGLS lines are in grey. Dashed black lines represent 95% confidence intervals and prediction inntervals of the PGLS lines. The gyrification index is strongly correlated with brain mass both across all mammals and within carnivores and canids. **a**) The gyrification index plotted against brain mass in all mammals with carnivores highlighted, lines represent the relationship across all mammals; **b**) The gyrification index plotted against brain mass in carnivores, with wild and domestic canids highlighted, lines represent the relationship for all carnivores with domestic canids excluded; **c**) The gyrification index plotted against brain mass in wild canids with the domestic canids overlaid. The lines represent the relationship for the wild canids; **d**) The gyrification index plotted against brain mass in a sample of domestic canids. Note, the weak regression statistics with only 3% of the variation in GI being explained by brain mass within the domestic dogs.

3.2. Inter and intraspecific scaling of global GI with brain mass in wild and domestic canids

To test whether domestic dogs underwent changes in scaling of GI relative to brain mass, we compared them with wild canids (e.g., wolves, foxes and coyotes). We conducted regression analyses for GI against brain mass based solely on the wild canid species and superimposed the domestic dog data points for visual comparison (Fig. ~~5~~6c). Regression

analysis of global GI against brain mass for the canids revealed a hypoallometric relationship between brain mass and GI (OLS slope = 0.19, $p < 0.001$, R-squared = 0.98; PGLS slope = 0.19, $p < 0.001$, R-squared = 0.90) with 90-98% of the variance in GI within the wild canids being explained by variation in brain mass. As shown in Figure ~~5c~~6c, the majority of the domestic dog data points lie well within the 95% prediction intervals. The mean GI for the domestic dog sample was also superimposed on the wild canid regression, and similarly lay well within the prediction and confidence intervals for the canid regression line (Fig. ~~5c~~6c).

Intraspecific scaling of global GI against brain mass for the sample of domestic dogs (Fig. ~~5d~~6d) revealed a low (non-significant), but still hypoallometric, relationship between brain mass and GI (OLS slope = 0.08, p =0.30, R-squared = 0.03); however, this analyses revealed that only 3% of the variance in GI within the domestic dog sample could be explained by variation in brain mass. Mean brain mass in this sample of domestic dogs was 73.12 g (range = 47.4g-112.2g, ~~Std.dev~~SD = 16.41, coefficient of variation = 22.4%). Mean GI in this sample of domestic dogs was 1.74 (range = 1.54-2.36, ~~Std.dev~~SD = 0.17, coefficient of variation = 9.81%).

3.3. Associations between GI and cortical grey and white matter volume, surface area and cortical thickness in canids

To evaluate the interspecific scaling of GI among canids, we computed regression analyses of global GI against cortical grey matter volume, surface area and cortical thickness in

the canidsae (Fig. 67, Table 2).

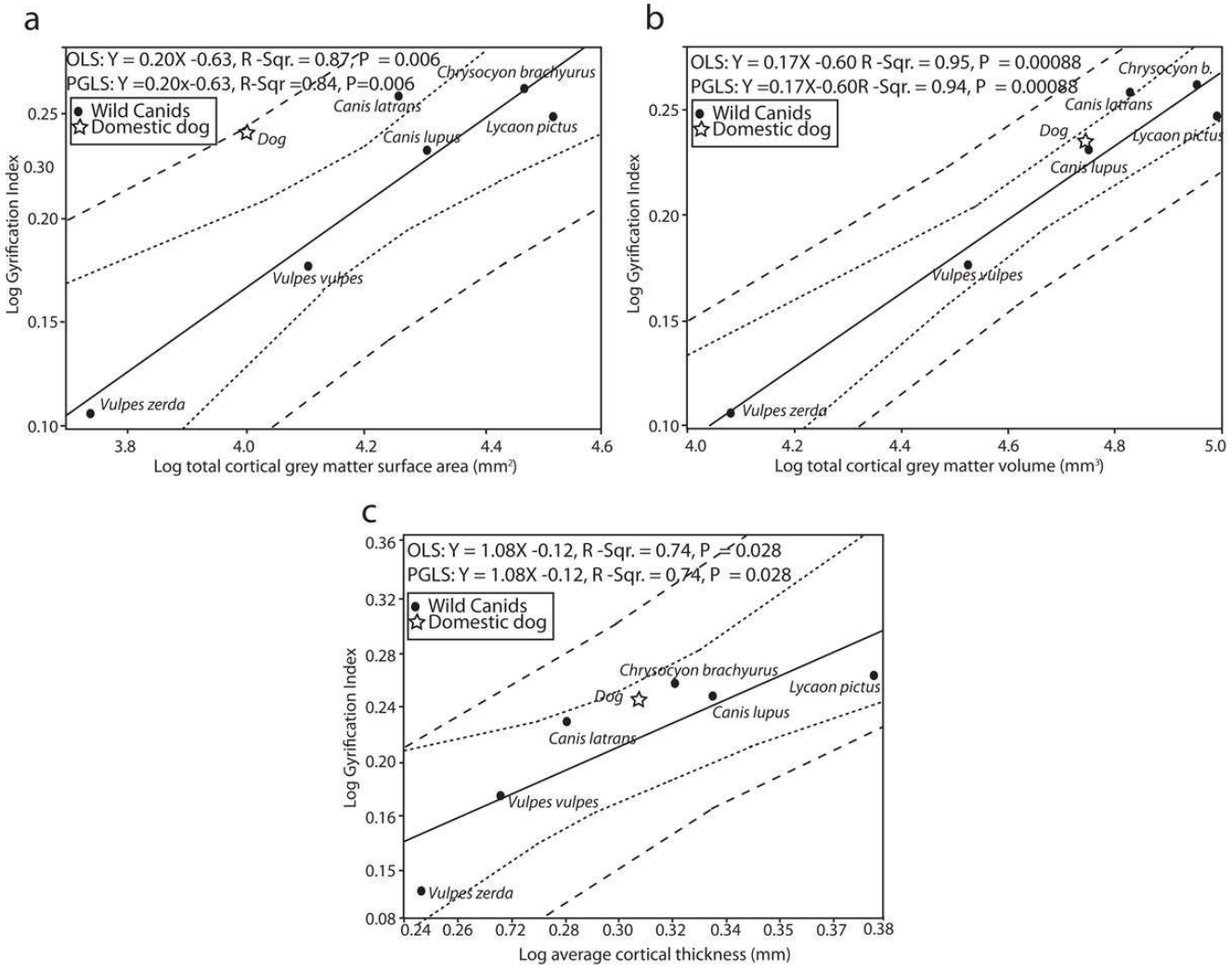

Figure 67: Regression analysis of gyrification index (Global) plotted against grey matter parameters across the six canid species. All data were logarithmically transformed (base 10) prior to inclusion in the regression analyses. Data used to derive these relationships are shown in Table 2. The domestic dog average was superimposed (star) onto that for the wild canids and was not included in computation of the interspecifc regression. **a**) The gyrification index plotted against total cortical grey matter surface area (mm^2); **b**) The gyrification index plotted against total

459 cortical grey matter volume (mm^3); **c**) The gyrification index plotted against average cortical
460 grey matter thickness (mm).

461
462
463 Regression analysis of grey matter surface area plotted against global GI for canids
464 revealed a hypoallometric relationship (OLS slope = 0.20, $p < 0.01$, R-squared = 0.87; PGLS
465 slope = 0.20, $p < 0.001$, R-squared = 0.84). A similarly hypoallometric pattern of change was
466 observed for the bivariate plot of cortical grey matter volume against global GI (OLS slope =
467 0.17, $p < 0.01$, R-squared = 0.95; PGLS slope = 0.17, $p < 0.001$, R-squared = 0.94). In contrast,
468 bivariate regression analysis of average cortical thickness against global GI for the canids was
469 characterized by a hyperallometric scaling pattern (OLS slope = 1.0819, $p < 0.051$, R-squared =
470 0.7492; PGLS slope = 1.0819, $p < 0.0501$, R-squared = 0.7940) with 7940% of the variance in
471 global GI accounted for by variance in average cortical thickness.
472 Interspecific scaling of the local GI against grey matter parameters (Table 3) revealed
473 similar results to that observed for global GI (Fig. 7a8a, b and Table 4).

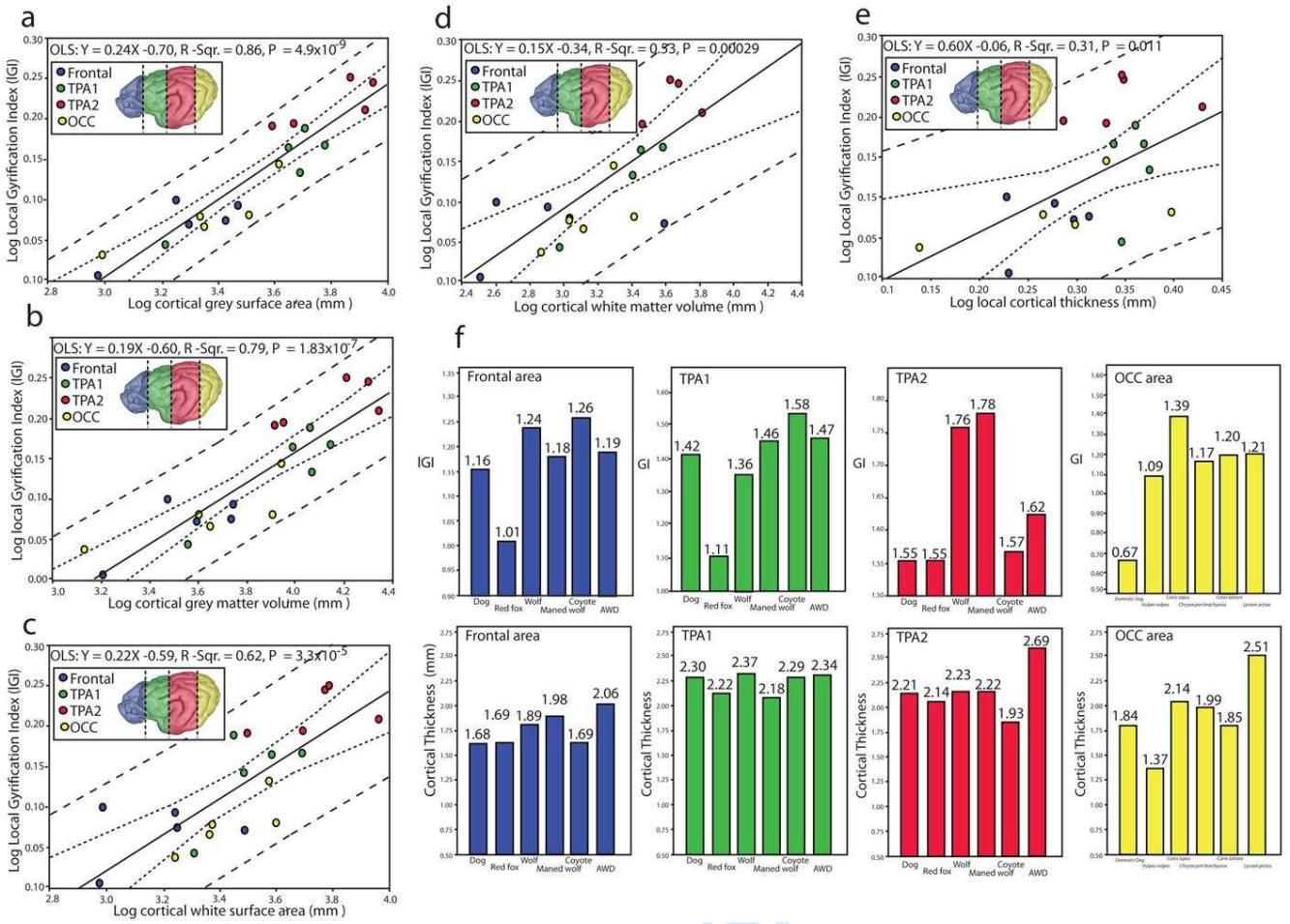

Figure 8: Regression analysis of the local gyrification index (lGI) plotted against grey matter parameters across the six canid species. All data were logarithmically transformed (base 10) prior to inclusion in the regression analyses. Data used to derive these relationships are shown in Table 3. The domestic dogs were not included in computation of the interspecifc regression. **a**) The local gyrification index plotted against total cortical grey matter surface area (mm^2); **b**) The local gyrification index plotted against total cortical grey matter volume (mm^3); **c**) The local gyrification index plotted against total cortical white matter surface area (mm^2); **d**) The local gyrification index plotted against total cortical white matter volume (mm^3); **e**) The local gyrification index plotted against local cortical grey matter thickness (mm); **f**) Bar graphs showing the species differences in local gyrification index (lGI) and cortical thickness in the Frontal, tempoparietal area (TPA1), tempoparietal area 2 (TPA2) and the occipital areas (OCC) as delineated using anatomical landmarks shown in Figure 3 and Figure 4b. AWD = African wild dog, Wolf = European wolf.

In particular, regression analysis of grey matter surface area and grey matter volume plotted against local GI was characterized by hypoallometric relationships (OLS slope = 0.24 – 0.19) with 86% and 79% of the variance in local GI explained by each parameter respectively.

Interspecific scaling of white matter parameters against local GI were similarly hypoallometric (Fig. ~~7e~~8c, d and Table 4) but were less strongly correlated with local GI than that observed for grey matter parameters (that is ~~i.e.,~~ regression statistics revealed that only 62% and 53% of the variance in local GI could be explained by variance in white matter surface area and volume respectively). Bivariate regression analysis of local cortical thickness against local GI revealed a similar significant hypoallometric scaling pattern (OLS slope = 0.60, $p < 0.01$, R-squared = 0.31), with 31% of the variance in local GI explained by local cortical thickness.

4. DISCUSSION

4.1. Inter- and intraspecific scaling of global GI with brain mass

The current study uses a phylogenetic comparative approach to investigate cortical gyrencephaly within the Carnivora in the context of other mammals (Zilles et al., 1989; Pillay & Manger, 2007~~;~~ Manger et al., 2012). As with earlier findings based on two-dimensional histological data (Welker, 1990; Zilles et al., 1989; Pillay & Manger, 2007; Manger et al., 2012), our results using a 3D approach confirm that mammals with larger brains tend to have more folded cortical surfaces. We demonstrate that this general pattern of an increase in cortical folding with an increase in brain size, is observed also within the carnivores and in the canid family. At these phylogenetic scales, changes in GI are characterized by a hypoallometric relationship (i.e., a slope < 1) indicating that the rate of GI increase is lower than that of brain mass. In earlier analyses of GI scaling in carnivores, Manger et al. (2012) and Pillay and

Manger (2007) demonstrated through the use of OLS regression analysis that GI was strongly predictable from brain mass. The authors observed a hypometric scaling relationship characterized by a slope of between 0.087-0.115 and a predictive capability of between 89-99% (Manger et al 2012; Pillay & Manger, 2007). Here using a larger dataset as well as PGLS methods to account for phylogeny, we observed a similar pattern of high predictability within the carnivores (slope = 0.10), with 87% of the variance in GI explained by variation in brain mass. The slight differences in regression statistics between OLS and PGLS indicate that scaling relationships are somewhat influenced by phylogenetic relationships between species. This hypoallometric relationship predicts that for every doubling of carnivore brain mass, carnivore GI is expected to increase by approximately 1.11 times which is similar to the 1.06 expected increase estimated by Manger et al. (2012). For the ~~Canidae~~canids, we observed a similar high predictability (98% of the variance in GI explained by variation in brain mass; slope = 0.19), with GI expected to increase by approximately 1.21 times for every doubling in canid brain mass.

This general pattern of hypoallometry was also observed in an intraspecific sample of domestic dogs, but our results indicate that the strength of this correlative relationship is dramatically reduced at this phylogenetic scale, with only 3% of the variance in GI being explained by variation in brain mass. It is possible that this reduction in predictive power could be result of human selection for a wider range of body sizes in domestic dogs, thus effecting the scaling attributes with GI through the indirect effect on the brain and body size relationship. However, in an earlier study on GI scaling in domestic dogs, Wosinski and colleagues (1996) demonstrated conclusively using multiple regression analysis that GI is almost exclusively determined by brain mass, with the partial correlation coefficient of GI with brain mass

markedly higher than that found for body weight or shoulder height in dogs (i.e., partial correlation coefficient for brain mass is 0.540, in comparison to 0.077 for body weight and 0.069 for shoulder height). This suggests that brain mass is a determinant factor in gyrification for domestic dogs and that GI is mimimally effected by body size differences (Wosinski Schleicher & Zilles, 1996).

Brain mass for our domestic dogs sampled ranged between 47.4g to 112.2g, almost a 2.5 fold difference in brain mass between the smallest (Dachsshund) and largest dog (~~Hungarian pointer~~Vizsla/ Hungarian pointer) breeds. While it is reasonable to expect that brachycephalic breeds should deviate from that of more typical dog breeds (Schoenebeck et al. 2012), we did not observe any clear patterns in scaling among brachycephalic breeds, likely a result of the limited representation of this group in the current sample. Given that the coefficient of variation in brain mass was 22.4 % in comparison to 9.81% for GI, it is evident that the greater dispersion of brain sizes contributes towards this reduction in the overall correlative power. The reduction in scaling parameters within domestic dogs is indicative of the greater intraspecific variation found at this phylogenetic scale, potentially as a result of domestication.

Variation in the scaling of cortical folding as a result of taxonomic differences~~,~~ have been reported in earlier studies. For example, Zilles et al. (1989) found that across primates, global GI values increased as a function of brain mass, but GI within a given species was not correlated with brain mass (Zilles et al., 1989). Our results align well with this earlier study, demonstrating that at higher taxonomic levels there exists a strong correlative relationship between GI and brain mass, but that this pattern quickly proceeds toward non-significance for comparisons within domestic dogs. Given that natural selection typically operates at the level of the population (within a given species), one could interpret the low intraspecific regression

558 statistics as suggesting that these static allometries in cortical folding are less constrained by
559 functional and or biophysical properties than that observed at higher taxonomic levels, leading
560 to greater variability in GI. Similarly, for domesticated animals such as the dog, one may argue
561 that these static allometries in gyrification are decoupled by the effect of artificial selection,
562 which has drastically pushed the upper and lower bounds of body mass (and associated brain
563 mass) within this group.
564
565 **4.2 Scaling of GI with grey matter volume, surface area and cortical thickness in canids**
566 We observed that cortical grey matter volume and surface area within canids scaled in a
567 hypoallometric fashion (slope range 0.18-0.23) with the gyrification index (both global and
568 local), such that canids with larger brains tended to have relatively less grey matter
569 volume/surface area than their diminutive counterparts and thus less folded cortices. This
570 pattern of scaling is congruent with that predicted in earlier studies (Manger et al., 2012). We
571 also observed differences in canid regression statistics between grey matter surface area scaling
572 with GI and grey matter volume scaling with GI. In particular, the rate of increase of cortical
573 grey matter surface area (slope = 0.199-0.235) was greater than the rate of increase for cortical
574 grey matter volume (slope = 0.175-0.189). This observation suggests that cortical folding within
575 the canids is likely to be constrained by the interplay of these two variables, such that increases
576 in surface area outpace any increase in volume resulting in a more folded cortical sheet relative
577 to volume, a finding first noted by Pillay and Manger (2007). Using a mathematical modelling
578 approach, Mota and Herculano-Houzel (2015) arrived at a similar conclusion, elegantly
579 demonstrating that the scaling of cortical folding was dependent on the lateral expansion of the

cortical sheet (i.e., surface area) relative to the underlying cortical thickness (i.e., grey matter volume).

Our results support this conclusion and suggest that this pattern holds true for the canids, thus expanding the observation of universal scaling. In addition, further evidence in support of this observation is the hyperallometric relationship displayed between cortical thickness and GI (slope =1.189) for the canidae, emphasizing that global cortical folding changes outpace changes in the underlying cortical thickness.

4.3 Scaling of local GI with white and grey matter volume and surface area in canids

According to Rakic's ~~(1988a, 1988b, 2004)~~ radial unit hypothesis (1988a, 1988b, 2004)~~,~~ an increase in cortical folding would result in a net increase in cortical surface area due to the subsequent addition of radial units (namely, cortical columns) to the expanding surface. Consequently, local cortical folding differences would thus more closely correlate to changes in the underlying grey matter as opposed to the white matter, as expansion of the cortical surface is facilitated by the addition of radial units spanning this underlying area. This prediction is consistent with our observations of local cortical grey and white matter scaling in canids. In particular, we observed that local GI scaling with cortical white matter parameters for the canids was consistently hypoallometric and that both white matter volume and surface area demonstrated significantly lower predictive power (50 and 61% of variance explained, respectively) than that observed for similar grey matter parameters (78 and 85% of variance explained, respectively).

603 **4.4 Variation in gyrification: possible functional implications and associated behavioral**
604 **ecology for canids**

605 We observed regional, as well as species, differences in gyrification of the cerebral
606 cortex in canids (both local and global; Fig. ~~7f~~ 8f and Table 4). These regional and species
607 differences in GI are likely reflective of rearrangements in the underlying cortical column as
608 predicted by the radial unit hypothesis (Rakic, 2004). There is evidence for regional and species
609 differences in cortical column morphology (e.g., Spocter et al., 2015; 2012; Raghanti et al.,
610 2010). For instance in anthropoid primates, minicolumn width ~~has been shown~~scales ~~to scale~~
611 with brain size (Spocter et al., 2015), coinciding with the general pattern of increasing cortical
612 folding observed in large-brained anthropoid species (Manger et al., 2013). Other examples
613 include the relative expansion of minicolumn width and neuropil space in the human
614 temporoparietal cortex (area Tpt), Broca's area and prefrontal cortex (Buxhoeveden &
615 Casanova, 2000; Buxhoeveden et al., 2001a,b; Schenker et al., 2008, Spocter et al., 2012),
616 reflective of the change in circuitry ~~towards~~ associated with human language specialization and
617 cognition. Furthermore, there is also strong evidence indicating that minicolumn morphology
618 (e.g., width and mean cell spacing) may vary naturally in a given population (Casanova, 2006)
619 and is linked to individual differences in cognition, as well as certain disease phenotypes (e.g.,
620 Casanova et al., 2007). Collectively, these observations suggest that rearrangements in the
621 cortical column as reflected through regional differences in cortical folding, may be indicative
622 of functional differences between canid species as well.

623 With the aim of advancing this hypothesis, we cautiously interpret our findings using
624 corresponding cortical maps for carnivores (Manger et al., 2008; Kroeneke et al., 2014; Sereno
625 & Allman, 1991; Chengetanai et al., 2020; see Fig. 3) and describe some of the relevant

behavioral ecology for each species. While the gross anatomical landmarks of the brain surface do not align sharply with cytoarchitectural boundaries, in the absence of cortical maps for the canids, this approach provides a working hypothesis for interpreting regional folding differences in this group.

In fact, we identified correspondence between our designation of the frontal region in canids, and the general location of the prefrontal cortex of carnivores (Fig. ~~3~~4). Similarly, we predict that the region we designate TPA1 overlaps with the putative primary motor area of canids, while the region TPA2 includes a large part of the somatosensory cortex, posterior parietal, auditory, posterior pseudosylvian and some ~~association~~ visual association areas. Also, as seen in the comparative cortical maps of the cat, ferret and African wild dog, the OCC region includes large parts of the putative canid visual cortex (i.e., it covers portions of the occipital, suprasylvian, and temporal visual regions). Below we describe three species--specific patterns of local GI variability that emerged from our study.

1) 'Fox-like' patterns of local GI variability. One of the patterns that emerges from our data was a separation of canids into what appeared to be two groupings, the one being a more 'fox-like' group and the other more 'wolf-like'. In particular, we observed low local GI values in the red fox (*Vulpes vulpes*), with this species having the lowest local GI for the frontal, anterior temporoparietal and posterior temporoparietal regions. In comparison, all other 'wolf-like' canid species clustered fairly close together in terms of local GI for these same regions. Given the relatively small folding index observed in the frontal region of the red fox in comparison to the other canids (Fig. ~~7f~~8f), we speculate that the underlying cortical column structure in foxes may be distinct from that observed in 'wolf-like'canids and that this has influenced the function of the putative prefrontal cortex of the fox. Similarly, we speculate that

649 the relatively low local GI values observed in the fox TPA1 and TPA2 is also indicative of
650 underlying microanatomical changes (relative to wolf-like canids) for these regions. Further
651 evidence in support of a divergent folding pattern for TPA1 between 'fox-like' and 'wolf-like'
652 canids, has been provided by comparative endocast studies (e.g., Radinsky, 1973; Lyras & Van
653 Der Geer, 2003; Lyras, 2009). These studies describe divergent sulcal patterning between 'fox-
654 like' and 'wolf-like' canids, resulting from species differences in the ansate and coronal sulci
655 bordering the cruciate sulcus (the sulcal landmark between the primary motor and primary
656 somatosensory cortices) (Lyras & Van Der Geer, 2003; Lyras, 2009).
657 This finding of a separation in folding complexity between the 'fox-like' and 'wolf-like'
658 canids parallels comparative behavioral observations, which indicate differences in social
659 cognition between these broad canid groups. For instance, within the canids there is a spectrum
660 of sociality from more solitary behavior, as seen in the red fox, to the communal behavior
661 observed in the wolf and African wild dog (Nowak, 2005; Kleiman, 1967). While red foxes can
662 be monogamous or live in groups of several vixens with a single male, they typically forage
663 alone, preying on small rodents and insects (Nowak, 2005). In contrast the African wild dog and
664 European wolf participate in a range of communal activities including communal hunting,
665 resting and feeding (Kleiman, 1967). It is worth noting that although the foxes have smaller
666 brain masses than the other canids included in this study, brain mass for the red fox (45g) is still
667 comparable to that of a small domestic dog (e.g., the Daschund with a brain mass 47g – 61 g),
668 indicating that the pattern observed here is not a result of brain size but rather a difference in
669 morphology. It remains to be seen whether this fox-like pattern can be generalized to other fox
670 species outside of the fox family (*Vulpini*). For example, the bat- eared fox (*Otocyon megalotis*)
671 has one of the smallest brain sizes in the Canidae (Boddy et al., 2012) but is known to exhibit

an array of social behaviors, including allogrooming, playing, and sleeping and resting in a communal fashion (Kleiman, 1967, Lamprecht, 1979).

2) 'Wolf-like' patterns of local GI variability. The second pattern to emerge from our data is the distinct 'wolf-like' pattern of GI variability which we interpret in the context of the social behavior of the canidae. For communal living to be successful, there must also be a reduction in intraspecific aggression (Wrangham, 2018), often mediated through the evolution of specialized communicative behaviors, relaying, for example, important information about social status to conspecifics (Kleiman, 1967). As a result, one might predict that the more social, pack-living canids would display some evidence of neural specialziations manifest in cortical folding (i.e., local GI) of higher-order association areas to support communal living. In this regard, we observed that the European wolf (and the maned wolf discussed later) was quite distinct from the other canids sampled in having the highest folding index for region TPA2, suggesting an elaboration of the underlying somatosensory, auditory and ~~association~~ visual association areas which likely play a vital role in some of the complex communicative and hunting behavior necessary for communal contact in wolves. Wolves are highly social pack hunters and use their group hunting strategy to bring down prey substantially larger than themselves (Bailey, Myatt, & Wilson (2013). While the coyote also hunts socially, communal hunts occur very infrequently and are quite distinct from that observed in wolves (Bekoff, 1977; McVey et al., 2013). Unlike the 'fox-like' canids, wolves live in large, organized packs (Mech & Boitani, 2003), which are similar to that observed in the African wild dog and dhole (*Cuon alpinus*), both of which have a similar hunting strategy (Hayward, Lyngdoh, & Habib, 2014; Hayward, et al., 2006). Other canids not included in this current study but which also frequently

form communal/pack hunting groups, are the bush dog ~~and dingo~~ (Sosnovskii, 1967). One exception to the above pattern is the maned wolf which, although it had a large GI in the TPA2 region, is considered a solitary species (Nowak, 2005). It is important to note though that although maned wolves are largely solitary, they still remain monogous and are perennially bonded (Deitz, 1984). The prevaliling argument is that the dispersed foraging strategy and increased territoriality in this group, evolved relatively recently (in the late Pleistocene) in response to changes in prey dispersion and constraints on energetic demands (Simpson, 1980; Burt, 1943).

Furthermore, pack-hunting canids like the wolf, also participate in communal feeding, which is quite distinct from the more competitive feeding seen in scavengers like the jackal and coyote (Kleiman, 1967). African wild dogs have expanded the typical communal feeding behavior seen in wolves, and developed ritualized feeding characterized by members of the pack (young and adult) inducing one another to regurgitate food using infantile begging postures, arguably helping to reinforce social cohesion in the group (Kuhme, 1965). Among pack living canids, communal vocalizations (e.g., howling) are also often observed in wolves, coyotes, African wild dogs, golden jackals and two feral canid varieties (dingos, New Guinea singing dogs) (Seitz, 1959, Kleiman, 1967). Kleiman (1967) describes two categories of howling behavior for the canids, 1) that which occurs face to face as observed in the wolves and coyote, 2) and that which appears to function mainly to maintain auditory contact with conspecifics at a distance, as observed in the the maned wolf (Brady, 1981) and Arctic fox. Given the role of auditory and visual cues in the behavioral ecology of these canids, it seems reasonable to conclude that some of the changes in cortical folding within region TPA2 (as

observed in the wolf) are reflective of changes in brain structure to support expanded auditory and visual function in these behaviors.

3) Dog distinctiveness in OCC GI. The third pattern to emerge from our data was the distinctiveness of the domestic dog occipital GI pattern from that observed in other canids. Given that our comparative cortical maps suggest that the OCC includes large parts of the putative canid occipital and temporal visual cortex, we interpret the low GI values in the domestic dog (Fig. ~~7~~8f) as evidence of a reduction relative to wild canids in the underlying visual areas. Some evidence in support of this hypothesis is provided through comparisons of the retina in wolves and domestic dogs. Wolves are known to posses a prominent retinal visual streak, which is less pronounced in domestic dogs (Miller & Murphy, 1995). In addition, wolves also have a higher number of ganglion cells in the retina than domestic dogs, endowing wolves with a higher visual acuity (Peichl, 1992a, b). When one takes into consideration the strong evidence that the visual system varies in a coordinated manner within a species (Andrews, Halpern & Purves, 1997), such that a reduction in size of the optic nerve is associated with a proportionate reduction in the size of the lateral geniculate nucleus as well as primary visual area of the cortex, it is likely that changes in the local GI of the dog visual areas coincide with observations of changes in their optic nerve and retina. We postulate, that despite this change towards a reduced GI in the OCC, domestic dogs are still able to read human social behaviour via visual cues as this behavior is facilitated by changes in the underlying cognitive machinery involved in social attentiveness (Hare & Tomasello, 2005) and not changes in visual acuity.

While the European wolf has the highest OCC folding index amongst the canids (Fig. ~~7~~8f), the close proximity of GI values within the other wild canids suggests that this pattern is

likely shared across the group and that the reduction in GI as seen in domestic dogs is a derived feature, possibly arising as a resulted of artificial selection.

Although all canids use some form of communicative signaling, there is evidence that some do appear to have expanded their visual signaling abilities relative to others. Shenkel (1947) highlights that the face and the hindquarters are two focal areas which have been specialized for visual signaling. Species-specific facial expressions, particular during agonistic encounters have been described in canids (Fox, Halperin & Kohn, 1976), with the more 'wolf-like' canids (e.g., wolves, coyote, and dingo) showing an elaboration of facial signaling abilities used to convey dominance or social rank to conspecifics (Fox, 1969). Likewise, in the hindquarters the tail may also be used for visual signaling as exemplified by recent studies of tail wagging in domestic dogs (Siniscalchi et al., 2013; Artelle, Dumoulin & Remchen, 2010), as well as the behavioral responses of dogs to tail wagging in robotic dogs (Reimchen & Leaver, 2008).

4.5. Conclusion

Given the links between the underlying cortical column and cortical folding, further comparative studies of cortical microstructure of the canids is needed, especially as it relates to comparisons of wild and domestic species. Although the current study is limited in sample size (i.e., the number of wild canid species) the current findings help to place domestic dog neuroanatomy into a phylogenetic context, both within the canids and broadly within the carnivores, which is necessary to contextualize the potential changes in canine brain evolution.

762

763 **References:**
764

765 Anderson, J.R., Sallaberry, P., & Barbier, H. (1995). Use of experimenter-given cues during
766 object-choice tasks by capuchin monkeys. *Animal Behavior* 49 (1), 201-208.
767 Doi:10.1016/0003-3472(95)80168-5

768

769

770 Spocter, M.A., Uddin, A., Ng, J.C., et al.(2018). Scaling of the corpus callosum in wild and
771 domestic canids: Insights into the domesticated brain. *J Comp Neurol* 526 (15), 2341–2359.
772 Doi:10.1002/cne.24486

773

774 Andrews, T.J., Halpern, S.D., & Purves, D. (1997). Correlated size variations in human visual
775 cortex, lateral geniculate nucleus, and optic tract. *J Neurosci*. 17 (8), 2859–2868.
776 Doi:10.1523/JNEUROSCI.17-08-02859.1997

777

778 Agnetta, B., Hare, B., & Tomasello, M. (2000). Cues to food location that domestic dogs (*Canis*
779 *familiaris*) of different ages do and do not use. *Animal Cognition* 3, 107-112. Doi:
780 10.1007/s100710000070

781

782 Artelle, K.A., Dumoulin, L.K., & Reimchen, T.E. (2009) Behavioral responses of dogs to
783 asymmetrical tail wagging of a robotic dog replica. *Laterality* 16 (2), 129-135. Doi:
784 10.1080/13576500903386700

785

Bailey, I., Myatt, J. P., & Wilson, A. M. (2013). Group hunting within the Carnivora: Physiological, cognitive and environmental influences on strategy and cooperation. *Behavioral Ecology and Sociobiology* 67, 1–17. Doi: 10.1007/s00265-012-1423-3

Bekoff, M. (1977). *Canis latrans*. *Mammalian Species* 79, 1–9. Doi: not available

Bensky, M. K., Gosling, S. D., & Sinn, D. L. (2013). The world from a dog's point of view: a review and synthesis of dog cognition research. *Advances in the Study of Animal Behaviour*, 45, 209-406. Doi: 10.1016/B978-0-12-407186-5.00005-7

Bininda-Emonds, O.R.P., Cardillo, M., Jones, K.E., MacPhee, R.D.E., Beck, R.M.D., Grenyer, R., Price, S.A., Vos, R.A., Gittleman, J.L., & Purvis, A. (2007). The delayed rise of present-day mammals. *Nature* 446, 507-512. Doi: 10.1038/nature05634

Bininda-Emonds, O.R.P., Cardillo, M., Jones, K.E., MacPhee, R.D.E., Beck, R.M.D., Grenyer, R., Price, S.A., Vos, R.A., Gittleman, J.L., & Purvis, A. (2008). Corrigendum. The delayed rise of present-day mammals. *Nature* 456, 274. Doi: 10.1038/nature07347

Boddy, A., McGowen, M., Sherwood, C., Grossman, L., Goodman, M., & Wildman, D. (2012). Comparative analysis of encephalization in mammals reveals relaxed constraints on anthropoid primate and cetacean brain scaling. *Journal of Evolutionary Biology*, 25(5), 981-994. Doi: 10.1111/j.1420-9101.2012.02491.x

Brady, C.A. (1981). The vocal repetoires of the bush dog (Speothos venaticus), crab-eating fox (*Cerdocyon thous*), and manned wolf (*Chryosyon brachyurus*). *Animal Behavior* 29 (3), 649-669. Doi: 10.1016/S0003-3472(81)80001-2

Brauer, J., Kaminski, J., Riedel, J., Call, J., & Tomasello, M. (2006). Making inferences about the location of hidden food: social dog, causal ape. *J Comp Psychol* 120, 38-47. Doi: 10.1037/0735-7036.120.1.38

Burt, W.H. (1943). Territoriality and home range concepts as applied to Mammals. *Journal of Mammology* 24, 346-352. Doi: 10.2307/1374834

Buxhoeveden, D., & Casanova, M.F. (2000). Comparative lateralization patterns in the language area of human, chimpanzee, and rhesus monkey brains. *Laterality* 5, 315–330. Doi: 10.1080/713754390

Buxhoeveden, D.P., Switala, A.E., Litaker, M., Roy, E., & Casanova, M.F. (2001a). Lateralization of minicolumns in human planum temporale is absent in nonhuman primate cortex. *Brain Behav Evol* 57, 349–358. Doi: 10.1159/000047253

Buxhoeveden, D.P., & Casanova, M.F.(2002a). The minicolumn and evolution of the brain. *Brain Behav Evol* 60,125–151. Doi: 10.1159/000065935

Buxhoeveden, D.P., & Casanova, M.F. (2002b). The minicolumn hypothesis in neuroscience. *Brain* 125, 935–951. Doi: 10.1093/brain/awf110

Buxhoeveden, D.P., Switala, A.E., Roy, E., Litaker, M., & Casanova, M.F. (2001b). Morphological differences between minicolumns in human and nonhuman primate cortex. *Am J Phys Anthropol* 115, 361–371. Doi: 10.1002/ajpa.1092

Casanova, M.F., Switala, A., Trippe, J., & Fitzgerald, M.(2007). Comparative minicolumnar morphometry of three distinguished scientists. *Autism* 11, 557–569. Doi: 10.1177/1362361307083261

Casanova, M.F. (2006). Neuropathological and genetic findings in autism: the significance of a putative minicolumnopathy. *Neuroscientist* 12, 435–441. Doi: 10.1177/1073858406290375

Chengetania, S., Bhagwandin, A., Bertelson, M, F., Hard, T., Hof, P.R., Spocter, M.A., & Manger, P.R (In Press). The brain of the African wild dog. IV. The visual system. *Journal of Comparative Neurology*.

Datta R, Lee J, Duda J, Avants BB, Vite CH, et al. (2012) A Digital Atlas of the Dog Brain. *PLOS ONE* 7(12): e52140. Doi:10.1371/journal.pone.0052140

Dietz, J.M. (1984). Ecology and Social Organization of the Maned Wolf (*Chrysocyon brachyurus*). Doctoral dissertation, Michigan State University, East Lansing, Michigan. Doi: 10.5479/si.00810282.392

Fox, M.W., Halperin, S., Wise, A. and Kohn, E. (1976), Species and Hybrid Differences in Frequencies of Play and Agonistic Actions in Canids. *Zeitschrift für Tierpsychologie* 40: 194-209. Doi:10.1111/j.1439-0310.1976.tb00932.x

Fox, M. (1969). The Anatomy of Aggression and Its Ritualization in Canidae: A Developmental and Comparative Study. *Behaviour 35* (3/4), 242-258. Doi: 10.1163/156853969X00224

Gautam, P., Anstey, K. J., Wen, W., Sachdev, P. S., & Cherbuin, N. (2015). Cortical gyrification and its relationships with cortical volume, cortical thickness, and cognitive

performance in healthy mid-life adults. *Behavioural brain research*, *287*, 331–339. Doi: 10.1016/j.bbr.2015.03.018.

Gregory, M. D., Kippenhan, J. S., Dickinson, D., Carrasco, J., Mattay, V. S., Weinberger, D. R., & Berman, K. F. (2016). Regional Variations in Brain Gyrification Are Associated with General Cognitive Ability in Humans. *Current biology : CB*, *26*(10), 1301–1305. Doi: 10.1016/j.cub.2016.03.021

Hare, B., Brown, M., Williamson, C., & Tomasello, M. (2002). The domestication of social cognition in dogs. *Science* 298,1634-1636. Doi: 10.1126/science.1072702

Hare, B., Call, J., & Tomasello, M. (1998). Communication of food location between human and dog (*Canis familiaris*). *Evolution of Communication* 2, 137-159. Doi: 10.1075/eoc.2.1.06har

Hare, B., & Tomasello, M. (2005). Human-like social skills in dogs? *Trends Cogn Sci* 9, 439-444. Doi: 10.1016/j.tics.2005.07.003

Hayward, M. W., Lyngdoh, S., & Habib, B. (2014). Diet and prey preferences of dholes. (*Cuon alpinus*): Dietary competition within Asia's apex predator guild. *Journal of Zoology* 294, 255–266. Doi: 10.1111/jzo.12171

Hayward, M. W., O'Brien, J., Hofmeyr, M., & Kerley, G. I. H. (2006).Prey preferences of the African wild dog Lycaon pictus (Canidae:Carnivora): Ecological requirements for conservation. *Journal of Mammalogy* 87, 1122–1131. Doi: 10.1644/05-MAMM-A-304R2.1

Hecht, E.E., Smaers, J.B., Dunn, W.D., Kent, M., Preuss, T.M., & Gutman, D.A. (2019). Significant Neuroanatomical Variation Among Domestic Dog Breeds. *Journal of Neuroscience* 39 (39), 7748-7758; Doi: 10.1523/JNEUROSCI.0303-19.2019

Itakura, S., Agnetta, B., Hare, B., & Tomasello, M. (1999). Chimpanzees use human and conspecific social cues to locate hidden food. *Developmental Science* 2,448-456. Doi: 10.1111/1467-7687.00089

Jardim-Messeder, D., Lambert, K., Noctor, S., et al.(2017). Dogs Have the Most Neurons, Though Not the Largest Brain: Trade-Off between Body Mass and Number of Neurons in the Cerebral Cortex of Large Carnivoran Species. *Front Neuroanat*. 2017;11:118. Doi:10.3389/fnana.2017.00118.

Jurney, C., Haddad, J., Crawford, N., Miller, A.D., Van Winkle, T.J., Vite, C. H., Sponenberg, P., Inzana, K.D., Crook, C.R., Britt, L., & O'Brien, D.P. (2009). Polymicrogyria in standard poodles. *Journal of Veterinary Internal Medicine* 23, 871-874.

Kleiman, D.G. (1967). Some aspects of social behavior in the Canidae. *Am. Zoologist* 7, 365-372. Doi: 10.1093/icb/7.2.365

Kroenke, C.D., Mills, B.D., Olavarria, J.F., & Neil, J.J.(2014). Neuroanatomy of the ferret brain with focus on the cerebral cortex. In J.G. Fox & R. P. Marini (eds.), *Biology and Diseases of the Ferret*, Third edition. John Wiley & Sons, Inc. Doi: 10.1002/9781118782699.ch3

Kruska, D. (1975). Comparative quantitative study on brains of wild and laboratory rats.I. Comparison of volume of total brain and classical brain parts. *J Hirnforsch* 16, 469-483. Doi: Not available.

Kruska, D. (1972). Volumetric comparison of various visual centers in the brains of wild boars and domestic pigs. *Z Anat Entwicklungsgesch* 138, 265-282. Doi: Not available.

965

966 Kruska, D. (1970). Comparative cytoarchitectonical investigations in brains of wild and
967 domestic pigs. *Z. Anat. Entwickl.-Gesch* 131, 291-324. Doi: Not available.

968

969

970 Kruska, D. & Schott, U. (1977) Comparative-quantitative investigations of brains of wild and
971 laboratory rats. *J Hirnforsch* 18, 59-67. Doi: Not available.

972

973

974 Kruska, D. & Stephan, H. (1973) Volumetric comparison of allocortical brain centers in wild
975 and domestic pigs. *Acta Anat (Basel)* 84, 387-415. Doi: Not available.

976

977 Kruska, D. (1973) Cerebralisation, Hirnevolution und domestikationsbedingte
978 Hirngrößenänderungen innerhalb der Ordnung Perissodactyla Owen, 1848 und ein Vergleich
979 mit der Ordnung Artiodactyla Owen, 1848. *J Zool Syst Evol Res* 11, 81-103. Doi:
980 10.1111/j.1439-0469.1973.tb00135.x

981

982 Kruska, V.D. (1980) Domestikationsbedingte Hirngrößenanderungen bei Säugetieren. *J Zool*
983 *Syst Evol Res* 18, 161-195. Doi: Not available.

Kuhme, W. (1965). Freilandstudien zur Soziologie des Hyanenhundes (*Lycaon pictus lupinus Thomas*, 1902). *Z. Tierpsychol* 22, 495-541. Doi: Not available.

Lamprecht, J. (1979). Field Observations on the Behaviour and Social System of the Bat-eared Fox *Otocyon megalotis Desmarest*. Zeitschrift für Tierpsychologie, 49(3), 260-284. Doi: 10.1111/j.1439-0310.1979.tb00292.x

Leergaard, T. B., White, N. S., de Crespigny, A., Bolstad, I., D'Arceuil, H., Bjaalie, J.G. & Dale, A. M. (2010) Quantitative histological nvalidation of diffusion MRI fiber orientation distributions in the rat brain. *PLoS ONE* 5 (1): e8595. Doi: 10.1371/journal.pone.0008595

Lin, L.I. (1989) A concordance correlation coefficient to evaluate reproducibility. *Biometrics* 45, 225-268. Doi: Not available.

Luders, E., Narr, K. L., Bilder, R. M., Szeszko, P. R., Gurbani, M. N., Hamilton, L., Toga, A. W., & Gaser, C. (2008). Mapping the relationship between cortical convolution and intelligence: effects of gender. *Cerebral cortex (New York, N.Y. : 1991)*, *18*(9), 2019–2026. Doi: 5510.1093/cercor/bhm227

Lyras, G.A. (2009). The evolution of the brain in Canidae (Mammalia: Carnivora). *Scr Geol* 139, 1–93. Doi: Not available.

Lyras, G.A. & Van der Geer, A.A.E. (2003). External brain anatomy in relation to phylogeny of Caninae (Carnivora: Canidae). *Zoological Journal of the Linnean Society* 138, 505-522. Doi: 10.1046/j.1096-3642.2003.00067.x

Manger, P.R., Spocter, M.A., & Patzke, N.(2013). The evolutions of large brain size in mammals: the 'over-700-gram club quartet'. *Brain Behav Evol* 82 (1), 68–78. Doi:10.1159/000352056

Manger, P.R., Engler, G., Moll, C.K., & Engel, A.K.(2008). Location, architecture, and retinotopy of the anteromedial lateral suprasylvian visual area (AMLS) of the ferret (Mustela putorius). *Vis Neurosci* 25 (1), 27–37. Doi:10.1017/S0952523808080036

Manger, P.R., Prowse, M., Haagensen, M., & Hemingway, J.(2012). Quantitative analysis of neocortical gyrencephaly in African elephants (Loxodonta africana) and six species of cetaceans: comparison with other mammals. *J Comp Neurol* 520 (11), 2430–2439. Doi:10.1002/cne.23046

Mangin, J.F., Riviere, D., Cachia, A., Duchesnay, E., Cointepas, Y., Papadopoulos-Orfanos, D., Collins, D.L., Evans, A.C., & Regis, J.(2004). Object-based morphometry of the cerebral cortex. *Medical Imaging*. 23, 968–982. [PubMed: 15338731]

Mangin, J.F.(2000). MMBIA. Hilton Head, South Carolina: IEEE Press; 2000. *Entropy minimization for automatic correction of intensity nonuniformity*; p. 162-169. Doi: Not available.

Mangin, J.F., Regis, J., & Frouin, V.(1996). Workshop on Mathematical Methods in Biomedical Image Analysis. San Francisco, CA: IEEE Press; 1996. *Shape bottlenecks and conservative flow systems*; p. 319-328. Doi: Not available.

Matsuda, Y., & Ohi, Y. (2018). Cortical gyrification in schizophrenia: current perspectives. *Neuropsychiatric Disease and Treatment* 14,1861-1869. Doi: 10.2147/NDT.S145273

McKinley, J., & Sambrook, T.D. (2000). Use of human-given cues by domestic dogs (*Canis familiaris*) and horses (*Equus caballus*). *Animal Cognition* 3, 13-22. Doi:10.1007/s100710050046

Mech, L. D., & Boitani, L. (2003). Wolves: Behavior, ecology, and conservation. *University of Chicago Press*. Chicago, IL. Doi: Not available.

Miklósi, Á., Polgárdi, R., Topál, J., & Csányi,V. (1998). Use of experimenter-given cues in dogs. *Animal Cognition* 1,113-121. Doi: 10.1007/s100710050016

Miller, P.E., & Murphy, C.J. (1995). Vision in dogs. *Journal of the American Veterinary Medical Association 207*, 1623-1634. Doi: not available

Mota, B., & Herculano-Houzel, S.(2015). Cortical folding scales universally with surface area and thickness, not number of neurons. *Science* 349 (6243), 74–77. Doi:10.1126/science.aaa9101

Nowak, R.M. (2005). Walker's Carnivores of the world. *Johns Hopkins University Press*, Baltimore, Maryland. Doi: not available

Nyakatura, K., & Bininda-Emonds, O.R.P. (2015). Updating the evolutionary history of Carnivora (Mammalia): a new species-level supertress complete with divergence time estimates. *BMC Biology* 10, 12. Doi: 10.1186/1741-7007-10-12

Peichl, L. (1992a). Morphological types of ganglion cells in the dog and wolf retina. *Journal of Comparative Neurology 324*, 590-602. Doi: 10.1002/cne.903240411

Peichl, L. (1992b). Topography of ganglion cells in the dog and wolf retina. *Journal of Comparative Neurology 324*, 603-620. Doi:10.1002/cne.903240412

1083 Pillay, P., & Manger, P.R. (2007). Order-specific quantitative patterns of cortical gyrification.
1084 *Eur J Neurosci*. 2007;25(9):2705–2712. Doi:10.1111/j.1460-9568.2007.05524.x
1085
1086 Plogmann, D., & Kruska, D. (1990). Volumetric comparison of auditory structures in the brains
1087 of European wild boars (*Sus scrofa*) and domestic pigs (*Sus scrofa f. dom*.). *Brain Behav Evol*
1088 35,146-155. Doi: 10.1159/000115863
1089
1090
1091 Radinsky, L.(1973). Evolution of the canid brain. *Brain Behav Evol* 7 (3), 169–202.
1092 Doi:10.1159/000124409
1093
1094 Raghanti, M.A., Spocter, M.A., Butti, C., Hof, P.R., & Sherwood, C.C. (2010). A comparative
1095 perspective on minicolumns and inhibitory GABAergic interneurons in the neocortex. *Front*
1096 *Neuroanat* 2010;4:3. Doi:10.3389/neuro.05.003.2010
1097
1098 Rakic, P.(1988a). The specification of cerebral cortical areas: the radial unit hypothesis. *Science*
1099 241, 170-6. Doi: 10.1126/science.3291116
1100
1101
1102 Rakic, P. (1988b). Defects of neuronal migration and the apathogenesis of cortical
1103 malformations. *Prog Brain Res* 73, 15-37. Doi: 10.1016/s0079-6123(08)60494-x
1104
1105

Rakic, P. (2004). Neuroscience: immigration denied. *Nature* 427 (6976), 685–686. Doi:10.1038/427685a.

Reimchen, T.E., & Leaver, S.D.A. (2008). Behavioral responses of Canid familiaris to different tail lengths of remotely-controlled life-size dog replica. *Behavior* 145 (3), 377-390. Doi:https://doi.org/10.1163/156853908783402894

Rogers, J., Kochunov, P., Zilles, K., et al.(2010). On the genetic architecture of cortical folding and brain volume in primates. *Neuroimage* 53 (3), 1103–1108. Doi:10.1016/j.neuroimage.2010.02.020

Röhrs, M., & Ebinger, P. (1978). Die Beurteilung von Hirngrößenunterschieden zwischen Wild- und Haustieren. *J Zool Syst Evol Res* 16, 1-14. Doi: 10.1111/j.1439-0469.1978.tb00916.x

Schaer, M., Ottet, M.C., Scariati, E., Dukes, D., Franchini, M., Eliez, S., & Glaser, B. (2013). Decreased frontal gyrification correlates with altered connectivity in children with autism. *Frontiers in human neuroscience*, *7*, 750. Doi: 10.3389/fnhum.2013.00750.

Schleifenbaum, C. (1973). The postnatal development of the brain of poodles and wolves (author's transl). *Z Anat Entwicklungsgesch* 141, 179-205. Doi: Not available.

Schenkel, R. (1947). Ausdrucks-Studien an Wolfen. *Behaviour* 1, 81-129. Doi: Not available.

Schenker, N.M., Buxhoeveden, D., Blackmon, W.L., Amunts, K., Zilles, K., & Semendeferi, K. (2008). A comparative quantitative analysis of cytoarchitecture and minicolumnar organization in Broca's area in humans and great apes. *J Comp Neurol* 510, 117–128. Doi: 10.1002/cne.21792

Schoenebeck, J.J., Hutchinson, S.A., Byers, A., Beale, H.C., Carrington, B. Faden, D.L., Rimbault, M., Decker, B., Kidd, J.M., Sood, R., Boyko, A.R., Fondon III, J.W., Wayne, R.K., Bustamante, C.D., Ciruna, B., & Ostrander, E.A. (2012). Variation of *BMP3* Contributes to Dog Breed Skull Diversity. *PLOS Genetics* 8(8): e1002849. Doi: 10.1371/journal.pgen.1002849

Seitz, A. (1959). Beobachtungen an handaufgezogenen Goldschakalen (Cam's aureus algirensis Wagner, 1843). *Z. Tierpsychol* 16, 747-771. Doi: 10.1111/j.1439-0310.1959.tb02190.x

Simpson, G.G. (1980). Splendid Isolations. *Yale University Press*. New Haven. Doi: Not available.

Siniscalchi, M., Lusito, R., Vallortigara, G., & Quaranta, A. (2013) Seeing left-or right-asymmetrical tail wagging produced different emotional responses in dogs. *Current Biology* 23(22), 2279-2282. Doi: 10.1016/j.cub.2013.09.027

1156 Spocter, M.A., Uddin, A., Ng, J., Wong, E., Wang, V.X., Tang, C., Wicinski, B., Haas, J.,
1157 Bitterman, K., Raghanti, M.R.,Dunn, R., Hof, P.R., Sherwood, C.C., Jovanovik, J., Rusbridge,
1158 C., & Manger, P.R (2018). Scaling of the corpus callosum in wild and domestic canids: Insights
1159 into the domesticated brain. *Journal of Comparative Neurology* 526 (15), 2341-2359.
1160 Doi:10.1002/cne.24486
1161
1162 Spocter, M.A., Hopkins, W.D., Barks, S.K., et al.(2012). Neuropil distribution in the cerebral
1163 cortex differs between humans and chimpanzees. *J Comp Neurol* 520 (13), 2917–2929.
1164 Doi:10.1002/cne.23074
1165
1166 Spocter, M.A., Raghanti, M.A., Butti, C., Hof, P.R., & Sherwood, C.C. (2015). The
1167 Minicolumn in a Comparative Context. In: Casanova, M & Opris, I (eds.) *Recent Advances on*
1168 *the Modular Organization of the Cortex*. Springer Publishing. Doi: 10.1007/978-94-017-9900-
1169 3_5
1170
1171 Seehaus, A., Roebroeck, A., Bastiani, M., Foncesca, L., Bratzke, H., Lori, N., Vilanova, A.,
1172 Goebel, R. & Galuske, R. (2015). Histological validation of high-resolution DTI in human post
1173 mortem tissue. *Front. Neuroanat*. 9:98. Doi: 10.3389/fnana.2015.00098
1174
1175 Sereno, MI., & Allman, J.M. (1991) Cortical visual areas in mammals. In A.G. Leventhal (ed.),
1176 *The Neural Basis of Visual Function*. London: Macmillan, pp. 160-172. Doi: Not available.

Sosnovskii, I. P. (1967) Breeding the Red dog or dhole *Cuon alpinus* at Moscow Zoo. Intern. *Zoo Yearbook* 7, 120-122. Doi: Not available.

Welker, W. (1990). Why does cerebral cortex fissure and fold? A review of determinants of gyri and sulci. In: Jones EG, Peters A, editors. *Cerebral cortex: vol 8b, comparative structure and evolution of cerebral cortex, part II*. New York: Plenum Press, p 3–110. Doi: Not available

Wosinski, M., Schleicher, A., & Zilles, K.(1996). Quantitative analysis of gyrification of cerebral cortex in dogs. *Neurobiology (Bp)* 4 (4), 441–468. Doi: Not available

Wrangham, R.W.(2018). Two types of aggression in human evolution. *Proc Natl Acad Sci U S A*. 115 (2), 245–253. doi:10.1073/pnas.1713611115. Doi: 10.1073/pnas.1713611115

Zilles, K., Armstrong, E., Moser, K.H., Schleicher, A., & Stephan, H. (1989). Gyrification in the cerebral cortex of primates. *Brain Behav Evol* 34 (3),143–150. Doi:10.1159/000116500.

Zilles, K., Armstrong, E., Schleicher, A., & Kretschmann, H.J. (1988). The human pattern of gyrification in the cerebral cortex. *Anat Embryol (Berl)* 179 (2),173–179. Doi:10.1007/bf00304699

~~Figure Legends:~~

Figure 1: Representative images showing 3D data from the domestic dog (first row) and European wolf (second row). The series of images outlines the image segmentation pipeline used in calculating the gyrification index both species. In Step 1 of processing the MR images are imported into BrainVisa where the Morphologist tool is used to delineate the grey and white matter subcomponents, followed by pial and white matter reconstruction and sulcal extraction (**a-d**). In Step 2 the pial and white matter mesh data is imported into MeshLab (**e-f**), where the GI is calculated as the ratio of the the surface area of the outer cerebral cortex (Scortex) divided by the surface area of the convex hull of the cerebral cortex(Sconvex) (**g**).

Figure 2: Representative lateral and dorsolateral images of the maned wolf brain showing the 3D partitioning approach used for slicing the 3D mesh data (i.e., grey and white matter surfaces) into anatomical subregions (frontal, TPA1, TPA2, OCC). To standardize the processing approach, each subject mesh file was vertically aligned in Slic3r and sectioned using the Cutting Tool. Cutting planes were placed perpendicular to the long axis of the vertically aligned hemisphere and anatomically defined sulcal landmarks were used for partitioning (**a-e**). Dorsal lateral views of the maned wolf brain showing screenshots of the vertical alignment and virtual sectioning/slicing tool of the hemisphere (**f- h**). After reslicing the pial mesh into subcomponents, the local GI (lGI) was calculated using the ratio of the pial surface area (in the region of interest) and the surface area of the convex hull for the subregion.

Figure 3: Comparative cortical maps of three closely related carnivore species, the domestic cat (Sereno & Allman, 1991), ferret (Manger et al 2008; Kroeneke et al., 2014) and African wild dog (Chengetania et al. 2020). The dashed vertical lines indicate the placement of the four

anatomical regions (frontal, TPA1, TPA2, OCC) from which local gyrification indices were sampled in the current study. Note the images are not drawn to scale.

Figure 4: Phylogeny used in the implementation of phylogenetic generalized least squares (PGLS). PGLS was performed using the caper package (Orme et al., 2013). The phylogeny was constructed using data based on the mammalian super-tree (Bininda-Edmonds et al., 2007, 2008) and a recent super-tree for the Carnivora (Nyakatura & Bininda-Emonds, 2015).

Figure 5: Regression analysis of the gyrification index (Global) plotted against brain mass in a range of mammals. All data were logarithmically transformed (base 10) prior to inclusion in the regression analyses. Data used to derive these relationships are shown in Table 1. OLS = ordinary least squares regression; PGLS = phylogenetic generalized least squares. OLS lines are plotted in black, PGLS lines are in grey. Dashed black lines represent 95% confidence intervals and prediction inntervals of the PGLS lines. The gyrification index is strongly correlated with brain mass both across all mammals and within carnivores and canids. **a**) The gyrification index plotted against brain mass in all mammals with carnivores highlighted, lines represent the relationship across all mammals; **b**) The gyrification index plotted against brain mass in carnivores, with wild and domestic canids highlighted, lines represent the relationship for all carnivores with domestic canids excluded; **c**) The gyrification index plotted against brain mass in wild canids with the domestic canids overlaid. The lines represent the relationship for the wild canids; **d**) The gyrification index plotted against brain mass in a sample of domestic canids. Note, the weak regression statistics with only 3% of the variation in GI being explained by brain mass within the domestic dogs.

Figure 6: Regression analysis of gyrification index (Global) plotted against grey matter parameters across the six canid species. All data were logarithmically transformed (base 10) prior to inclusion in the regression analyses. Data used to derive these relationships are shown in Table 2. The domestic dog average was superimposed (star) onto that for the wild canids and was not included in computation of the interspecife regression. **a)** The gyrification index plotted against total cortical grey matter surface area (mm^2); **b)** The gyrification index plotted against total cortical grey matter volume (mm^3); **c)** The gyrification index plotted against average cortical grey matter thickness (mm).

Figure 7: Regression analysis of the local gyrification index (lGI) plotted against grey matter parameters across the six canid species. All data were logarithmically transformed (base 10) prior to inclusion in the regression analyses. Data used to derive these relationships are shown in Table 3. The domestic dogs were not included in computation of the interspecifc regression. **a)** The local gyrification index plotted against total cortical grey matter surface area (mm^2); **b)** The local gyrification index plotted against total cortical grey matter volume (mm^3); **c)** The local gyrification index plotted against total cortical white matter surface area (mm^2); **d)** The local gyrification index plotted against total cortical white matter volume (mm^3); **e)** The local gyrification index plotted against local cortical grey matter thickness (mm); **f)** Bar graphs showing the species differences in local gyrification index (lGI) and cortical thickness in the Frontal, tempoparietal area (TPA1), tempoparietal area 2 (TPA2) and the occipital areas (OCC) as delineated using anatomical landmarks shown in Figure 2 and Figure 3b.

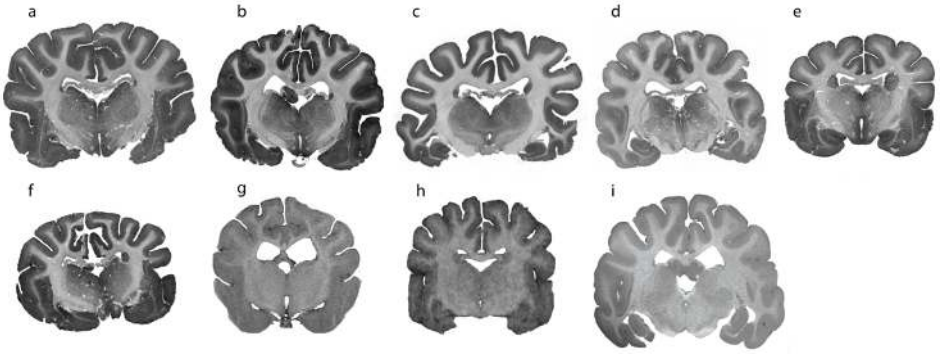

Figure 1: Representative coronal images through the diecephalon of select canid species used in the current study. a = African wild dog; b = Domestic dog; c = Maned wolf; d = coyote; e = red fox; f = fennec fox; g = domestic dog; h = domestic dog; i = European wolf. Scan a- f were obtained through scanning at the Department of Radiology, Icahn School of Medicine at Mount Sinai. Scan g is that of a domestic dog (Cavalier King Charles spaniel) scanned through collaboration with the University of Surrey and Fitzpatrick Referrals Ltd. Scan h is that of a domestic dog acquired through the MRI image data repository of Dr. Geoffrey Aguire at University of Pennsylvannia. Scan i was acquired through collaboration with the Department of Radiology at Oxford University.

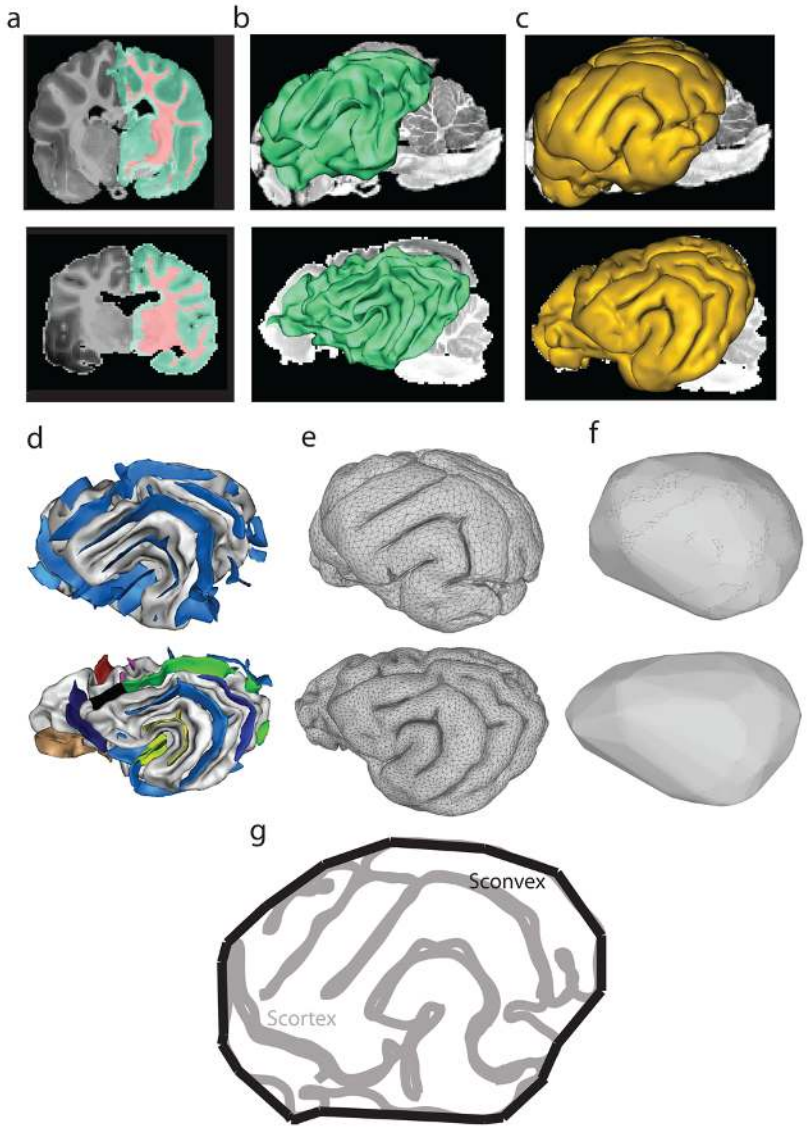

Figure 2: Representative images showing 3D data from the domestic dog (first row) and European wolf (second row). The series of images outlines the image segmentation pipeline used in calculating the gyrification index in both species. In Step 1 of processing, the MR images are imported into BrainVisa where the Morphologist tool is used to delineate the grey and white matter subcomponents, followed by pial and white matter reconstruction and sulcal extraction (a-d). In Step 2, the pial and white matter mesh data is imported into MeshLab (e-f), where the GI is calculated as the ratio of the the surface area of the outer cerebral cortex (Scortex) divided by the surface area of the convex hull of the cerebral cortex(Sconvex) (g).

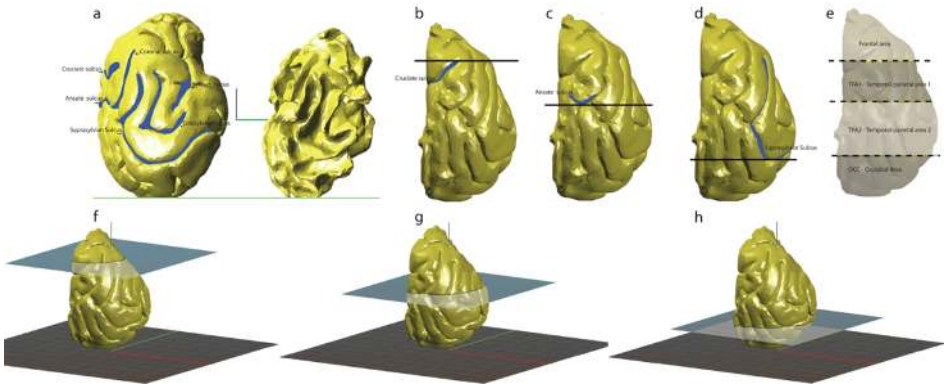

Figure 3: Representative lateral and dorsolateral images of the maned wolf brain showing the 3D partitioning approach used for slicing the 3D mesh data (i.e., grey and white matter surfaces) into anatomical subregions (frontal, TPA1, TPA2, OCC). To standardize the processing approach, each subject mesh file was vertically aligned in Slic3r and sectioned using the Cutting Tool. Cutting planes were placed perpendicular to the long axis of the vertically aligned hemisphere and anatomically defined sulcal landmarks were used for partitioning (a-e). Dorsal lateral views of the maned wolf brain showing screenshots of the vertical alignment and virtual sectioning/slicing tool of the hemisphere (f- h). After reslicing the pial mesh into subcomponents, the local GI (lGI) was calculated using the ratio of the pial surface area (in the region of interest) and the surface area of the convex hull for the subregion.

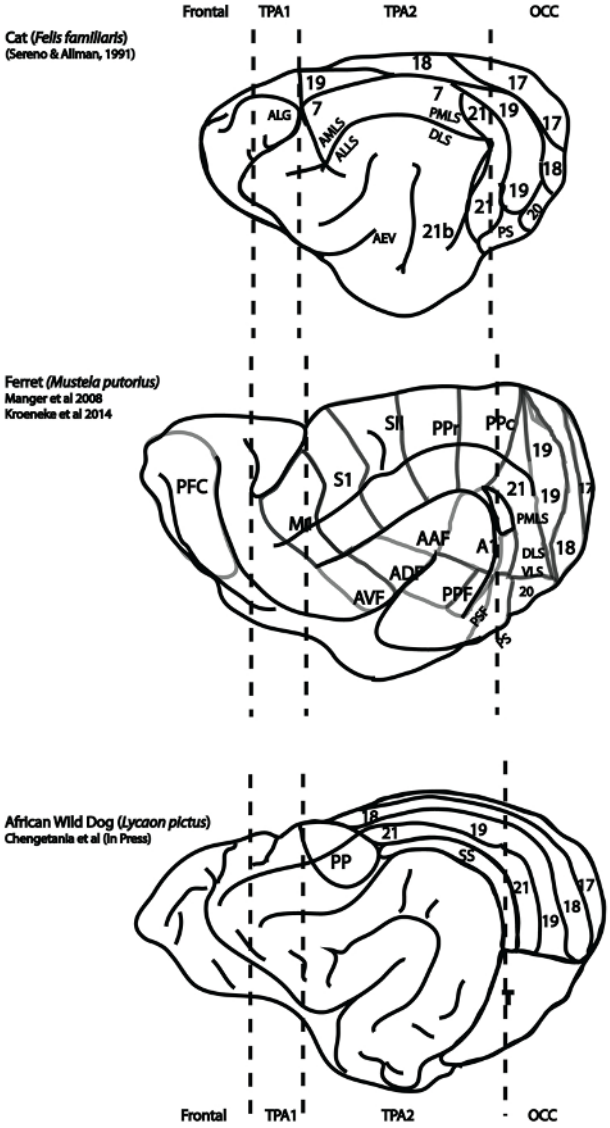

Figure 4: Comparative cortical maps of three closely related carnivore species, the domestic cat (Sereno & Allman, 1991), ferret (Manger et al 2008; Kroeneke et al., 2014) and African wild dog (Chengetania et al. 2020). The dashed vertical lines indicate the placement of the four anatomical regions (frontal, TPA1, TPA2, OCC) from which local gyrification indices were sampled in the current study. Note the images are not drawn to scale.

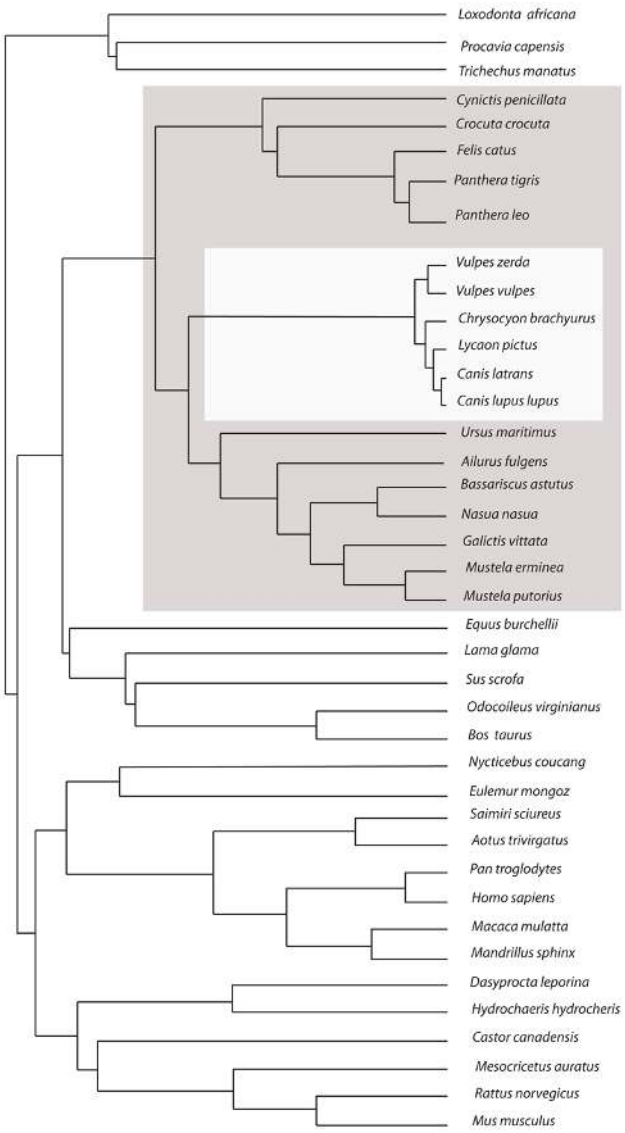

Figure 5: Phylogeny used in the implementation of phylogenetic generalized least squares (PGLS). PGLS was performed using the caper package (Orme et al., 2013). The phylogeny was constructed using data based on the mammalian super-tree (Bininda-Edmonds et al., 2007, 2008) and a recent super-tree for the Carnivora (Nyakatura & Bininda-Emonds, 2015).

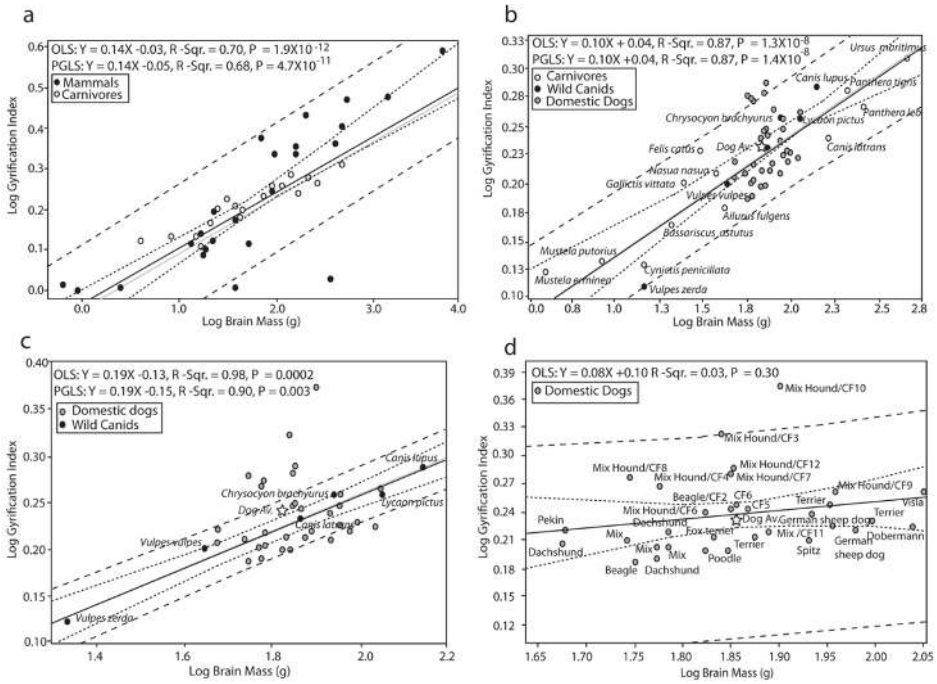

Figure 6: Regression analysis of the gyrification index (Global) plotted against brain mass in a range of mammals. All data were logarithmically transformed (base 10) prior to inclusion in the regression analyses. Data used to derive these relationships are shown in Table 1. OLS = ordinary least squares regression; PGLS = phylogenetic generalized least squares. OLS lines are plotted in black, PGLS lines are in grey. Dashed black lines represent 95% confidence intervals and prediction inntervals of the PGLS lines. The gyrification index is strongly correlated with brain mass both across all mammals and within carnivores and canids. a) The gyrification index plotted against brain mass in all mammals with carnivores highlighted, lines represent the relationship across all mammals; b) The gyrification index plotted against brain mass in carnivores, with wild and domestic canids highlighted, lines represent the relationship for all carnivores with domestic canids excluded; c) The gyrification index plotted against brain mass in wild canids with the domestic canids overlaid. The lines represent the relationship for the wild canids; d) The gyrification index plotted against brain mass in a sample of domestic canids. Note, the weak regression statistics with only 3% of the variation in GI being explained by brain mass within the domestic dogs.

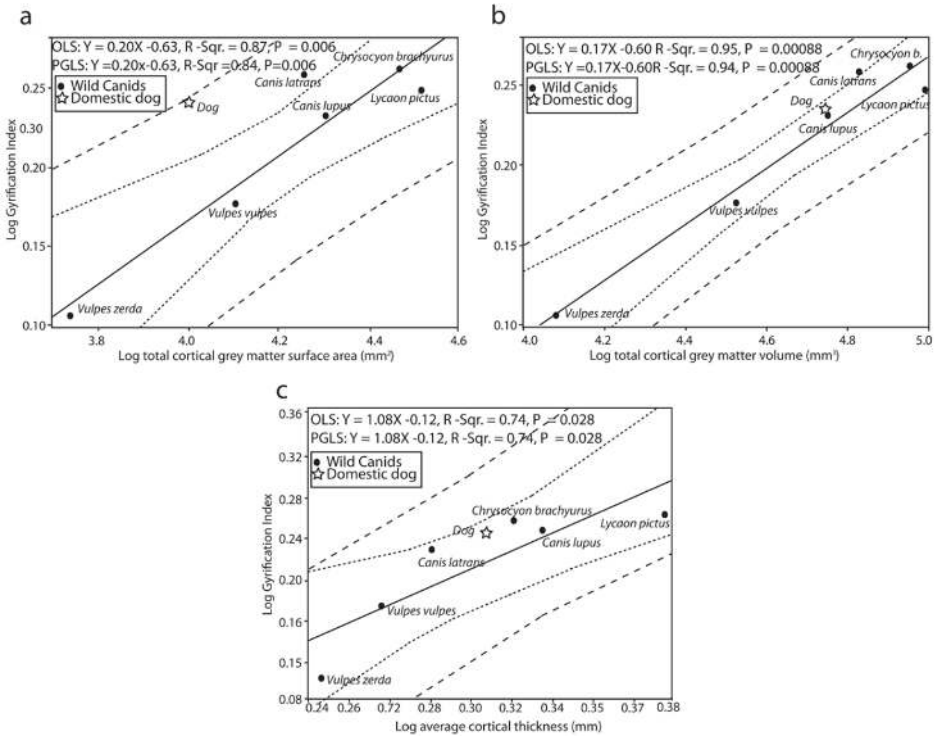

Figure 7: Regression analysis of gyrification index (Global) plotted against grey matter parameters across the six canid species. All data were logarithmically transformed (base 10) prior to inclusion in the regression analyses. Data used to derive these relationships are shown in Table 2. The domestic dog average was superimposed (star) onto that for the wild canids and was not included in computation of the interspecifc regression. a) The gyrification index plotted against total cortical grey matter surface area (mm2); b) The gyrification index plotted against total cortical grey matter volume (mm3); c) The gyrification index plotted against average cortical grey matter thickness (mm).

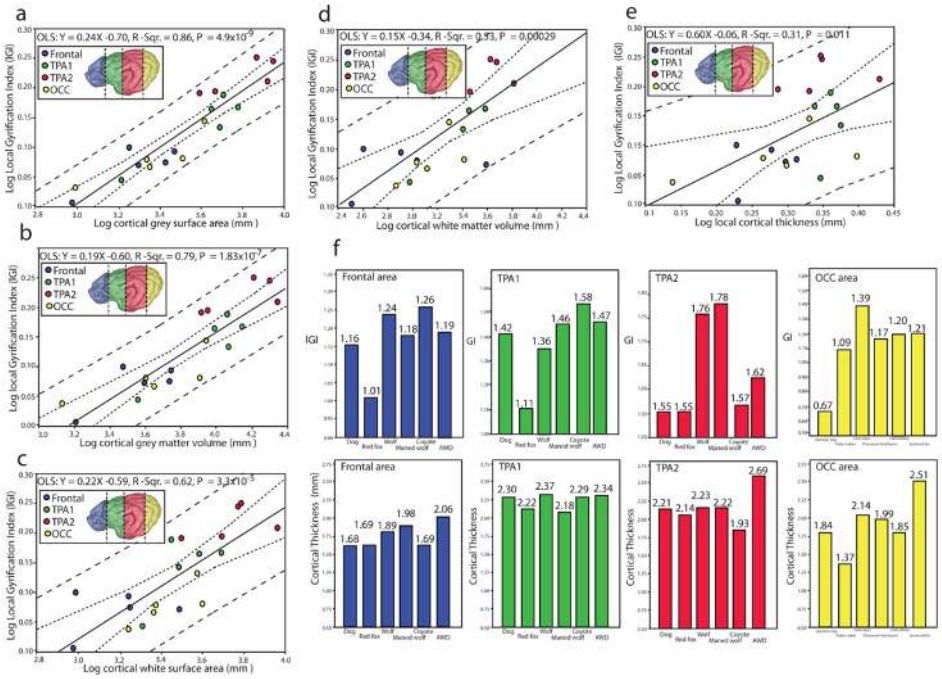

Figure 8: Regression analysis of the local gyrification index (lGI) plotted against grey matter parameters across the six canid species. All data were logarithmically transformed (base 10) prior to inclusion in the regression analyses. Data used to derive these relationships are shown in Table 3. The domestic dogs were not included in computation of the interspecifc regression. a) The local gyrification index plotted against total cortical grey matter surface area (mm2); b) The local gyrification index plotted against total cortical grey matter volume (mm3); c) The local gyrification index plotted against total cortical white matter surface area (mm2); d) The local gyrification index plotted against total cortical white matter volume (mm3); e) The local gyrification index plotted against local cortical grey matter thickness (mm); f) Bar graphs showing the species differences in local gyrification index (lGI) and cortical thickness in the Frontal, tempoparietal area (TPA1), tempoparietal area 2 (TPA2) and the occipital areas (OCC) as delineated using anatomical landmarks shown in Figure 3 and Figure 4b. AWD = African wild dog, Wolf = European wolf.